



Cite this: *J. Mater. Chem. B*, 2023,  
11, 955

## A review on borate bioactive glasses (BBG): effect of doping elements, degradation, and applications

Oluwatosin David Abodunrin, Khalil El Mabrouk \* and Meriame Bricha

Because of their excellent biologically active qualities, bioactive glasses (BGs) have been extensively used in the biomedical domain, leading to better tissue–implant interactions and promoting bone regeneration and wound healing. Aside from having attractive characteristics, BGs are appealing as a porous scaffold material. On the other hand, such porous scaffolds should enable tissue proliferation and integration with the natural bone and neighboring soft tissues and degrade at a rate that allows for new bone development while preventing bacterial colonization. Therefore, researchers have recently become interested in a different BG composition based on borate ( $B_2O_3$ ) rather than silicate ( $SiO_2$ ). Furthermore, apatite synthesis in the borate-based bioactive glass (BBG) is faster than in the silicate-based bioactive glass, which slowly transforms to hydroxyapatite. This low chemical durability of BBG indicates a fast degradation process, which has become a concern for their utilization in biological and biomedical applications. To address these shortcomings, glass network modifiers, active ions, and other materials can be combined with BBG to improve the bioactivity, mechanical, and regenerative properties, including its degradation potential. To this end, this review article will highlight the details of BBGs, including their structure, properties, and medical applications, such as bone regeneration, wound care, and dental/bone implant coatings. Furthermore, the mechanism of BBG surface reaction kinetics and the role of doping ions in controlling the low chemical durability of BBG and its effects on osteogenesis and angiogenesis will be outlined.

Received 16th November 2022,  
Accepted 29th December 2022

DOI: 10.1039/d2tb02505a

[rsc.li/materials-b](http://rsc.li/materials-b)

## 1. Introduction

*“If you can make a material that will survive exposure to high energy radiation, can you make a material that will survive exposure to the human body?”* was a question posed during a cordial dialogue involving professor Larry Hench and a returnee US Army colonel from Vietnam. This question led to the discovery of bioactive glass “45S5” trademarked Bioglass®, making it the very first simulated biomaterial to be scientifically confirmed to bond to bones.<sup>1,2</sup> The findings sparked a healthcare transformation and set the stage for current biomaterial-driven tissue regeneration, which is utilized to treat bone defects, dental deformities, and wounds as a result of its outstanding biocompatibility, as well as osteoconduction and osteoinduction qualities.<sup>3</sup> Iconic Larry Hench Bioglass® is a silicate-based BG comprised entirely of silicon dioxide, sodium dioxide, calcium dioxide, and phosphorus pentoxide that has been known for almost 54 years to bond to bone and soft tissue, as well as being one of the most commonly used materials for tissue regeneration. But even so, a significant focus is

already on using borate, phosphate, and other bioactive glass-doped systems as an extracellular matrix for biomedical applications.<sup>1,4</sup>

In orthopedic and maxillofacial applications, bone grafting procedures such as autograft, allograft, and xenograft (see Fig. 1A–C) are generally considered the gold standard for bone tissue engineering (BTE) treatments, as they provide a long-term restorative solution by vascularizing, integrating, and stimulating local bone healing. Despite their advantages, autografts have a fundamental limitation: they cause a structural defect at the donor site, resulting in subsequent severe morbidity and a low supply of autogenous bone. Other therapeutic options, such as allografts and xenografts, also pose a risk of infectious disease transmission, extra costs, ethical issues, and immunological rejection of the bone.<sup>5–12</sup> Alternatives to these grafting treatments include three-dimensional porous materials (scaffolds), injectable particles, and pastes made of synthetic and natural biomaterials (see Fig. 1D) that can increase bioactivity and osteo properties while providing mechanical support for bone regeneration.<sup>13–15</sup>

Silicate-based BGs and glass-ceramics, in particular, have gained a lot of interest for application in bone replacement and repair, along with wound healing processes, due to their inorganic origin, biomechanical strength, and physical

*Euromed Research Centre, Euromed Polytechnic School, Euromed University of Fes, Eco-Campus, Fes-Meknes Road, 30030 Fes, Morocco.*  
*E-mail: k.elmabrouk@euromed.org*

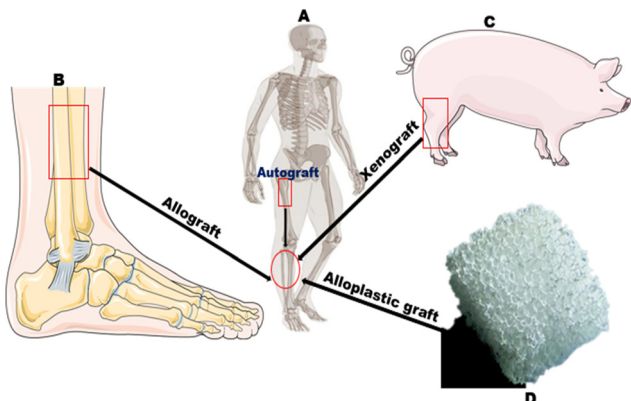


Fig. 1 Schematic overview of bone grafting procedures: (a) autograft (b) allograft (c) xenograft (d) alloplastic graft. "Figure modified with text, markings, and annotation after adaptation from Servier Medical Art by Servier, licensed under a Creative Commons Attribution 3.0 Unported License" (<https://creativecommons.org/licenses/by/3.0/>).

attributes that are reasonably near to hard tissues.<sup>16</sup> The dissolution of this glass network happens when it comes into contact with the biological environment, resulting in the production of a silica-rich layer on the glass surface, characterized by the development of an amorphous calcium phosphate apatite layer. With the proper adjustments, this sequence of reactions, commonly recognized for silicate BGs, is also applicable for BBGs; however, instead of silica gel, a borate-rich layer emerges.<sup>16–18</sup> Since the formation of a calcium phosphate apatite layer is associated with the BG's good adhesion with nearby bony structures and soft tissue. The frequency at which the BG gets converted to the apatite phase offers a threshold for assessing a material's *in vitro* bioactivity.<sup>19</sup> Even though SBF-based *in vitro* experiments show that BGs have good bioactivity, they are considered inadequate to estimate *in vivo* conditions.<sup>20</sup> Moreover, the requirements of cell culture experiments vary greatly and rely on how BG compositions will be used. Nonetheless, *in vitro* investigations utilizing various cell types, assays, and *in vivo* animal models are therefore required to assess the bioactivity of these BGs.<sup>21–25</sup>

According to their high bioactivity and slow degradation process, silicate-based BGs like 45S5 and 13-93 are slowly absorbed and undergo incomplete transformation to an apatite after implantation.<sup>26–28</sup> For instance, the borate equivalent of 45S5 BG designated as 45S5-3B, while immersed in simulated body fluid (SBF), converts swiftly and practically thoroughly around 3–4 days, unlike 45S5, which took many weeks to convert nearly 50% of it into HAP layers. As a result, their *in vitro* breakdown is relatively slow, which limits their use in biological applications.<sup>29–31</sup> On the other hand, the rapid pace of BBG degradation and transformation to HAP can ostensibly impair their ability to match the regrowth of new bone cells. Furthermore, this rapid degradation could weaken the physico-mechanical qualities and have an inefficiently guiding impact on the creation of new bone.<sup>32</sup> As a result, by regulating the glass composition, materials with appropriate bioactivity and regulated degradation behavior are needed to match the host

bone's replacement of the BG scaffolds through a moderate and complete dissolution of the implanted biomaterial.<sup>33,34</sup> Recent findings have shown that a significant amount of research is being conducted to develop borate/borosilicate BG by partial or complete substitution of the silica ( $\text{SiO}_2$ ) content with borate ( $\text{B}_2\text{O}_3$ ), leading to decreased chemical durability, a rapid and complete transition of the BG to HAP, and as such easily controlled degradation and bioactivity characteristics.<sup>35–40</sup> Furthermore, the body's faster transition of the BG to HAP is considered beneficial because the implant material can be removed entirely by the body system more quickly.<sup>41</sup> In addition to replacing  $\text{SiO}_2$  with  $\text{B}_2\text{O}_3$ , factors such as BG particle size of different diameters<sup>42,43</sup> and incorporation of active ions such as copper,<sup>43,44</sup> aluminium,<sup>45</sup> strontium,<sup>46</sup> sodium,<sup>47</sup> zinc,<sup>48</sup> magnesium,<sup>49</sup> lithium,<sup>50</sup> etc. into the BG system contribute to decreased chemical durability and ion release. Furthermore, ions delivered directly off an implant instead of systemically injected drugs have the benefits of being delivered where desired, resulting in better pharmacological efficacy and reduced side effects.<sup>51</sup>

The synthesis of borate/borosilicate BGs have been the subject of extensive investigation. In addition, multiple studies have emphasized the methods for BBGs production and degradation and their doping with different therapeutic ions, which positively affects angiogenesis and bone remodeling. To highlight a few, Kaur *et al.*<sup>17,52</sup> published an article/book that largely outlined the needs for BGs, their proportions, the structure-property interaction regarding hydroxyapatite deposition, the synthesis of metallic glasses and doped BGs, as well as the methods employed for their manufacture. The processing of BBGs, behavior *in vitro*, and the impact of boron ion release from BBGs on cell viability were all recently covered by Ege *et al.*<sup>53</sup> in their article. The biological effects of boron and the ability of the bioactive borate glass to regenerate both hard and soft tissues were also discussed by Seiji *et al.*<sup>54</sup> in a recent book chapter. Finally, an assessment of the use of metallic ions in tissue engineering and regenerative medicine is given in another manuscript by Viviana *et al.*<sup>55,56</sup> with a focus on their therapeutic uses and the requirement to develop methods for the release of loaded ions from biomaterial substrates.

Even though the regeneration of both soft and hard tissues has been intensively investigated with bioactive glass, the impacts of dopants on BBGs regarding slowing down the rate of fast degradation have received comparatively less attention. In actuality, the majority of review papers that have been written up to this point only cover a portion of the subject and ignore other vital contributions related to how dopants affect the main osteogenic characteristics of boron-containing BG composition. In light of this, this paper aims to give a general overview of doping ions' function, significance, and impacts on BBGs. This study begins with a description of BBGs, highlighting several characteristics while concentrating on these glasses' chemistry, nomenclature, and structure. Following, we'll talk about the reaction mechanism of BBGs, which is also the bone-bonding property of this sort of BG in physiological fluids. More particularly, the focus will be placed on the mechanism by which these doping ions regulate the BBG's

dissolution rate to keep up with bone growth and the dopant impacts on important osteogenic features. Finally, the paper's conclusion outlines BBG's application fields and future potential.

## 2. Borate bioactive glass (BBGs)

Borate-based glass is a type of inorganic glass with boron element as the network-forming precursor and can be directly absorbed into the shape of various structural elements inside the glass network. On the other hand, Boron is a trace mineral element ranging from 3–20 mg, found in the human body system, that has been shown in studies to play an essential role in wound healing, bone formation, and bone formation maintenance. Similarly, data suggests that boron also regulates steroid hormone development and action, which helps avoid calcium shortage and bone demineralization.<sup>57–59</sup> Moreover, boron is used in compositions including borate/borosilicate glass for tissue engineering because of its chemical reactivity and coefficient of thermal expansion (CTE), which prevents strong thermal shock resistance inside the glass network.<sup>60</sup> In this regard, boron ions in BG for bone formation and renewal release in the human body are significantly relevant.

45S5 silicate compositions have been studied extensively for many years. Still, borate- and borosilicate-based compositions, in which  $B_2O_3$  replaces a portion of  $SiO_2$  as the primary glass-forming agent, have only lately been investigated due to the trivalent electronic structure of boron, which differs from the quadrivalent structure of silicon.<sup>62</sup> This incorporation resulted in various physicochemical and biological properties of BBGs, as proven through the fast degradation mechanism (see Fig. 2) and cellular reactions concerning silica-based BG.<sup>61</sup> The phenomenon of  $BO_3$  triangles and  $BO_4$  tetrahedra coordination that constitutes a continuous system of vitreous boric oxide is an exciting feature of the borate glass structure; besides, as

more and more of these units assemble, they constitute well-defined and stable borate groups, such as diborate, triborate, and tetraborate, that also form the glass networks.<sup>63,64</sup> In contrast to silicate or phosphate glass, adding a certain molar percentage of alkali ions  $R_2O$  (where R can be Li, Na, or K) to  $B_2O_3$ -based glasses alters the network model by decreasing the boroxol rings. This disrupts the boroxol shape, shifting the boroxol ring vibration from around  $790\text{ cm}^{-1}$  to  $806\text{ cm}^{-1}$  regions in the Raman spectra.<sup>65</sup>

Consequently, Nuclear magnetic resonance (NMR) measurements reveal that depending on the type and concentration of  $R_2O$ , the transition of boron coordination from triangular to tetrahedral units takes place at a rate of 35–40 mol%  $R_2O$ ,<sup>66,67</sup> with further research indicating that the number of  $BO_4$  units increases until it reaches a maximum value of a specific  $R_2O$  concentration. However, when the addition of  $R_2O$  is more than 45 mol% concentration, reversal of  $BO_4$  to  $BO_3$  and characteristics such as increment in the number of non-bridging oxygen (NBO) ions are noticed.<sup>68</sup> Furthermore, as the network depolymerizes, ring and chain isomers of trigonal metaborate can be identified, and further depolymerization leads to the formation of pyroborate dimers and, eventually, orthoborate groups (see Fig. 3). This unique characteristic of continuous change in borate properties is referred to as the boron anomaly.<sup>17,64,69–73</sup>

Besides the boron anomalies, vitreous  $B_2O_3$  has several distinct features from vitreous  $SiO_2$  (see Table 1). The same applies to binary  $R_2O$ - $B_2O_3$  and  $R_2O$ - $SiO_2$  glasses. In particular, the polymerization process affects Borate glass's solubility and thermal characteristics due to an initial network increment from 3 to 4. Glass transition temperature ( $T_g$ ) increases, and a reversal happens at more significant modifier concentrations, decreasing  $T_g$ . This is not the case in a thermally and chemically stable silica glass network.<sup>63,64</sup> According to Du *et al.* study,<sup>75</sup> the B–O–Si– bond in typical borosilicate glass with four-coordinated boron can be broken easily as well as considerable phase separation occurs because the bond energy is relatively weak than that of

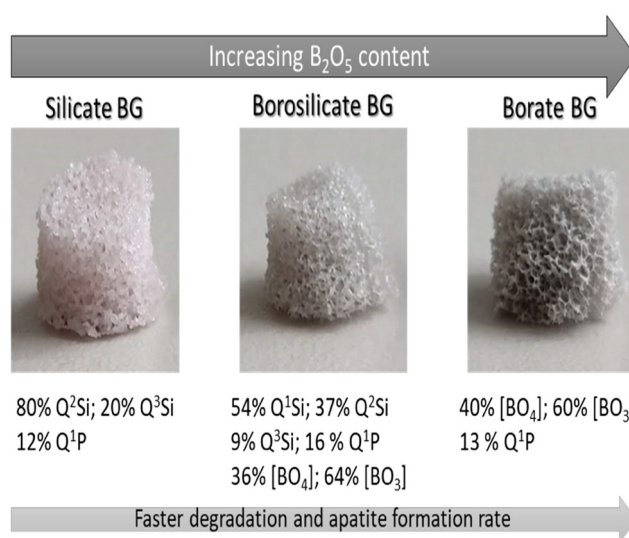


Fig. 2 Properties of the silicate, borosilicate, and borate BGs.<sup>61</sup> Licensed under a Creative Commons Attribution Non-Commercial 4.0 International (CC BY-NC 4.0) (<https://creativecommons.org/licenses/by-nc/4.0/>).

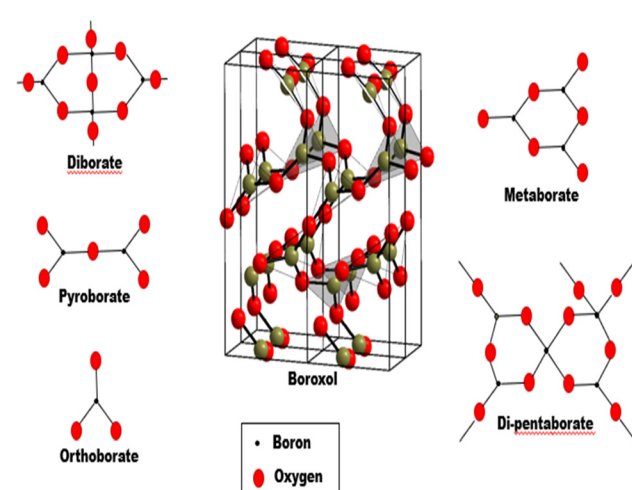


Fig. 3 Superstructural units found in borate glass system. "Boroxol structure is adapted from ref. 74, licensed under a Creative Commons Attribution 3.0 Unported License" (<https://creativecommons.org/licenses/by/3.0/>).

Table 1 Properties of vitreous  $B_2O_3$  against  $SiO_2$ 

Properties	$B_2O_3$ Value	$SiO_2$ Value	Ref.
Average network connectivity	3	4	73
Glass mass density, $d$ ( $g\ cm^{-3}$ )	1.844	2.2020	64
Crystalline mass density $d_x$ ( $g\ cm^{-3}$ )	2.5544	2.3179	64
Glass number density $\rho^0$	0.01595	0.022070	64
Crystalline number density $\rho_x^0$	0.022095	0.023232	64
Network number density $\rho_n^0$	0.03190	0.022070	64
Oxygen atom number density $\rho_o^0$	0.04785	0.044140	63,64
Trigonal covalent bond energy/strength (meV)	-5160		90
Tetrahedral covalent bond energy/strength (meV)	-3860	-4600	90
Crystallization from the melt at ambient $p$	No	Yes	91
Crystalline melting point, $t_m$ (K)	-3.8	-2.3	92
Glass transition temperature, $t_g$ (K)	553	1463	92
Bulk modulus, $k$ (GPa)	12.12	36.89	93
Shear modulus, $g$ (GPa)	6.85	31.03	93
Compressive strength	5-7	11	38 and 94
Young's modulus, $E$ (GPa)		35	94
Thermal expansion, $\alpha$ ( $10^{-7}\ K^{-1}$ ; 20–100 °C)	97–161.6	5.35–15.1	95–97
Thermal conductivity ( $W\ m^{-1}\ K^{-1}$ )	0.52	1.38	98
Specific heat at 295 K, $c_p$ ( $J\ mol^{-1}\ K^{-1}$ )	62.38	44.07	99

three-coordinated boron. This research shows that when modifier oxides are first introduced, the solubility of borate glass reduces, and the thermal characteristics are also altered. Solubility increases as the modifier content increase due to a more depolymerized borate structure with trigonal  $BO_3$  groups.<sup>75,76</sup> Omar *et al.*<sup>77,78</sup> Synthesized and evaluated silica-based and BBGs in terms of mechanical properties necessary for their use as metallic coating materials. It was discovered that BBGs have a Coefficient of Thermal Expansion (CTE) that is closer to the substrate's (Ti6Al4V) CTE, resulting in greater mode I significant strain energy release rates of glasses and compressive residual stresses and strains at the coating/substrate interface that perform better than their silica-based glasses equivalents. Another work by Leonie *et al.*<sup>79</sup> provides evidence that borate inclusion increases the BG's mechanical stability and bioactivity. This led to a modulus of 13–16 GPa, which is just marginally lower than that of compact bone, and a hardness of roughly 1 GPa, which is not excessively strong for BTE applications.

In addition to their Physico-chemical characteristics, BBGs have also shown excellent bioactive behaviour compared to silicate BGs in terms of biological characteristics.<sup>80,81</sup> Using human mesenchymal stem cells (hMSCs) and osteoblasts made from hMSCs (hMSC-Obs), Nicholas *et al.*<sup>82</sup> examined the cytocompatibility of borate glass in *in vitro* cell culture. The findings showed that these cell lineages survived up to two weeks after being seeded on porous borate glass disks, indicating that porous borate glass is effective at enhancing the expression of the early osteogenic marker while facilitating a favourable environment for cell attachment and proliferation. In a different study by Fabian *et al.*<sup>83</sup> the viability, proliferation, and osteogenic differentiation of human mesenchymal stromal cells were assessed *in vitro* using 0106-B1, a borate-based BG, and 45S5-BG. Accordingly, an *in vivo* test was also performed on scaffolds built from both BGs integrated with stromal cells and infused into mice to analyse osteoid development and angiogenic characteristics. Results demonstrated that there was a comparable effect of 45S5-BG and 0106-B1-BG on osteogenic

differentiation, proliferation, and viability. However, in terms of the quantity and maturity of the osteoid created *in vivo*, 0106-B1-BG-based scaffolds proportionately surpassed 45S5-BG-based scaffolds. Conversely, 0106-B1-BG demonstrated much higher angiogenic gene expression patterns than 45S5-BG, making 0106-B1-BG a more viable choice.

### 3. Mechanism of degradation process (surface reaction kinetics)

The progressive degradation of implanted biomaterials and simultaneous substitution of the implants by natural bone is required for bone regeneration applications. However, unlike wholly resorbable biomaterials, bioactive silicate glasses do not degrade entirely following implantation. Borate-based BG, on the contrary, due to the reduced network connectivity of trigonal planar  $[BO_3]$  and tetrahedral  $[BO_4]$  units in BBGs, has already been proven to have poor chemical stability and transition fast to calcium phosphate in dissolution media.<sup>38,84</sup> As a result, developing biomaterials having significant bioactivity and a controlled degradation rate to match the growing pace of bone *in vivo* is crucial.

Upon interaction with a bodily solution, HAP is deposited on the surface of BGs in a series of stages akin to the bone mineral phase.<sup>85,86</sup> To explain this phenomenon, the European Society for Biomaterials (in 1987) defined bioactive material as "*a material which has been designed to induce specific biological activity*".<sup>87</sup> Because of their ability to chemically attach to living bone by creating a bone-like HAP layer at the implant-bone interface, BGs are extremely attractive bone substitutes in bone regeneration.<sup>88</sup> However, the ability of a material to be coated by a HAP layer when interacting with physiological fluids has been proposed as a sign of bioactivity, and to evaluate the bioactivity of a BG material, ethics would not permit evaluating every new material directly in animals for experimental research, and it may not be economically sustainable. In this

regard, bioactivity tests with blood plasma buffered aqueous solution, and simulated body fluid (SBF) have proven to be an effective way to propose a tangible mechanism that explains the bioactive bond formation, influencing the development of new bioactive materials and allowing for the selection of the best biomaterials to continue development.<sup>89</sup>

BG behaviors in cells and animals are a more convincing way to demonstrate the bone-bonding phenomenon than buffer solutions, which are also an excellent technique to describe bioactivity. As an illustration, a pertinent work by Miquel *et al.*<sup>100</sup> examined the possible use of a borosilicate BG scaffold as a bone substitute material and demonstrated bioactive behavior in SBF, osteoblast (MC3T3-E1) cell, and animal model. First, two BG scaffolds were pre-treated with SBF to encourage the development of distinct bone-like apatite layers on their surfaces. Based on the surface examination and material characterization, both SBF-treated scaffolds had a layer of carbonated hydroxyapatite (HCA) that was calcium deficient. Following this, MC3T3-E1 cells were seeded onto the scaffolds. Analysis showed that MC3T3-E1 pre-osteoblasts displayed a more flattened shape and cell proliferation in the untreated scaffold.

On the other hand, SBF-treated samples had longer, more osteoblastic active cells. Results from *in vivo* experiments using a rabbit calvarial bone deficiency model revealed that SBF pre-treated scaffolds promoted bone growth more effectively than untreated ones. Cui and colleagues<sup>101</sup> created an injectable borate bioactive glass cement in their other applicable work. Borate glass was changed into HAP over 25 days when this material was cultured in phosphate-buffered saline. Moreover, the injectable BBG cement developed in this study was incorporated in rabbit tibial defects infected with methicillin-resistant *Staphylococcus aureus*. The material transformed to HA and promoted new bone formation in the defects within 8 weeks, clearly showing that it is a promising treatment for osteomyelitis and regeneration of bone with defects.

The bioactivity process, first proposed by Hench for silicate glasses, can be thought of as a sort of glass corrosion guided by complex glass–fluid interactions governed by inorganic chemicals (stages 1–5) and biological (stages 6–12) mechanisms.<sup>102</sup> This sequence of reactions is commonly recognized for silicate BGs and is also applicable for borate BGs with correct adjustments; nevertheless, instead of silica gel, a borate-rich layer emerges in step 3.<sup>39</sup>

Primarily, a vast amount of triangle-shaped  $[\text{BO}_3]$  and tetrahedral  $[\text{BO}_4]$  functional units are linked during the formation of the BBG network structure, whereas the modifier  $\text{M}^+$  (metal) cations inside this glass, such as  $\text{Na}^+$ ,  $\text{K}^+$ , and  $\text{Mg}^{2+}$ , suffice to stabilize the net charge of the bridged oxygen ions. The leaching process begins with the dissolving of  $\text{Na}^+$  ions and, most certainly,  $\text{Ca}^{2+}$  from the glass surface into the solution, while the glass's B–O network is affected by the phosphate solution (see Fig. 4). Cations and  $\text{OH}^-$  levels rise as a result. The reaction equations below show that  $\text{H}^+$  created during water hydrolysis disrupts the glass network structure, yielding water-soluble  $\text{B}(\text{OH})_3$  or  $\text{B}(\text{OH})_4$ .<sup>30,103</sup>

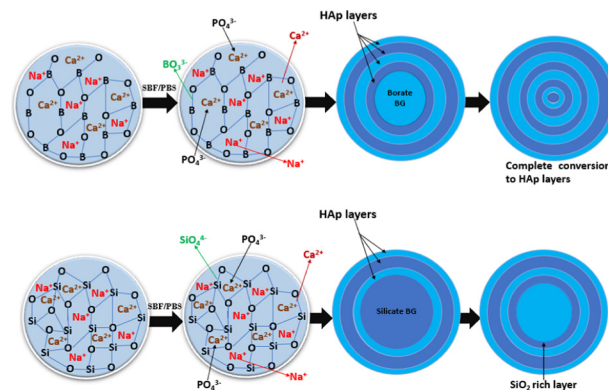


Fig. 4 Degradation process of borate and silicate bioactive glass.



After the borate network on the glass surface is disrupted, the  $\text{PO}_4^{3-}$  ions in the dissolution medium react with  $\text{Ca}^{2+}$  ions on the glass surface, prompting the nucleation of HAP. Subsequently, the created HAP can permeate additional  $\text{PO}_4^{3-}$  ions through its channels, reacting with the  $\text{Ca}^{2+}$  sites beneath it to generate an additional layer of HAP.

This continual dissolution–precipitation process yields numerous layers of HAP that lower the glass–solution interaction until the aggregate borate glass is transformed into HAP. Moreover, in the case of borate glasses containing silicate as a co-network former, the dissolution–precipitation reaction stops before complete conversion to HAP, leaving a residual or dissolvable  $\text{SiO}_2$ -rich gel layer within reaction products. This subsequently slows the degradation of borosilicate BG.<sup>26,104</sup> Typically, for a borate glass like 13-93B3, the conversion is regulated by an interfacial reaction, and the kinetics can be modelled as a 3-D contracting sphere. Therefore, the conversion of a silicate glass, such as 13-93, is somewhat influenced primarily through reactions at the interface (3-D contracting sphere model) and subsequently by ion diffusion to the reaction interface (3-D diffusion model).<sup>105</sup> Essentially, a reaction occurs on the surface of the sphere in the contracting sphere model (see Fig. 5), which is usually referred to as a moving interface model. Regarding BG, the particles, whether they are a single particle or a group of particles, have a sphere-shaped core made of unreacted material that gradually decreases in size, encircled by the shell(s) of the product.<sup>106,107</sup>

Huang *et al.*'s research<sup>30</sup> extensively characterize the conversion of multiple glasses, including a bioactive silicate glass (45S5), a borate equivalent of 45S5 glass with all of the  $\text{SiO}_2$  in 45S5 glass replaced with  $\text{B}_2\text{O}_3$ , as well as two intermediate borosilicate glass mixtures. The only principal constituents within the precipitate for the borate equivalent of 45S5 BG comprised oxides of calcium ( $\text{CaO}$ ) and phosphorus ( $\text{P}_2\text{O}_5$ ), showing that the glass was almost wholly converted to HAP. Meanwhile, experimental results show that  $\text{CaO}$ ,  $\text{P}_2\text{O}_5$ , and  $\text{SiO}_2$  are the core constituents of the reaction products for the silicate and borosilicate BG. Although, within 4 days, particles of a borate glass could ultimately convert to HAP. Even after

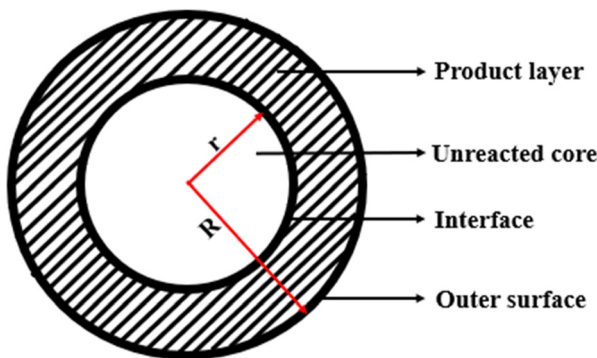


Fig. 5 Contracting sphere model illustration of reacting bioactive glass.

70 days, 45S5 glass particles and two intermediate borosilicate formulations of the same mass were only partially transformed to HAP. As a result, the existence of unreacted  $\text{SiO}_2$  indicates that the degradation process of BG can be controlled by adjusting the amount of  $\text{B}_2\text{O}_3$ .<sup>30,35</sup> Chandrani *et al.* conducted a study that further supported the accelerated degradation rate of BBG. According to their findings, the ion exchange activity of BBG after immersion in SBF was attributed to the rapid discharge of  $\text{Ca}^{2+}$ ,  $(\text{PO}_4)^3-$ , and  $(\text{BO}_3)^3-$  ions, as well as the initiation of amorphous calcium phosphate within shells formed upon SBF interaction. This dissolution process shows that the scaffold's percent weight loss was most significant on the first day and intensified with SBF soaking time.<sup>108</sup> In a related study, Liu *et al.* examined the efficacy of using BBG scaffolds to release medications to treat bone infections. More than 90% of the glass in the scaffolds is dissolved after a week to produce poorly crystallized hydroxyapatite, according to an *in vitro* degradation of the pellets and their transformation to a hydroxyapatite-type in an SBF medium.<sup>109</sup>

## 4. Doping ions' role in regulating BBG degradation rate and osteogenic biomarkers

### 4.1. Copper

Numerous copper (Cu)-containing biomaterials have been researched and created recently due to copper's significant benefits.<sup>110–112</sup> Conversely, it has been shown that Cu promotes angiogenesis (see Fig. 6), stimulates endothelial cell development, and makes it easier for vascular endothelial growth factor to be released (VEGF). Besides, research has also shown that incorporating Cu increases the stability of borosilicate and borate glasses, modifying their characteristic features and bioactivity and increasing the antibacterial activity of BG. Therefore, to enhance their applications, it is crucial to understand how Cu, as a dopant, affects the characteristics of BGs. Additionally, understanding how materials degrade is essential for managing the biological performance of BG and its derived scaffolds and determining how released ions interact with cells.<sup>44,112–114</sup>

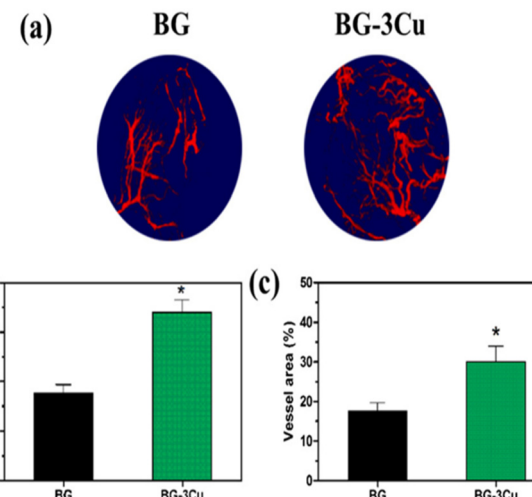


Fig. 6 (a) 3D reconstructions of the new blood vessels implanted with Cu-doped BG show higher blood vessel density in the defect implant than with the undoped BG. (b and c) evaluation of Cu ion on the extent and quantity of newly formed blood vessels. Image adapted from ref. 44 with permission from Elsevier.

The phenomenon of the Cu doping impacts on the BBG during the degrading phase can be thought of in terms of the electronegativity, oxygen coordination number, and ionization energy of the dopant cations. Cu ions are therefore integrated into the glass network matrix through octahedral coordination and act as network modifiers in the glass system.<sup>115</sup> Wang *et al.*<sup>44</sup> Looked into how copper dopant influenced the borosilicate glass network's structural characteristics and how the derived glass scaffolds' reactivity and degradation behavior changed. The research's findings showed that the pairing of  $\text{BO}_2\text{O}^-$  units, as well as non-bridging oxygen (NBO), transition to  $\text{BO}_4$  units. This was enhanced by the doping Cu, which NBO surrounded.

Consequently, as the proportion of Cu doping in the glass system increased, more  $\text{BO}_4$  groups were formed, creating a more stable structure, which led to a reduced boron ion release rate in the dissolution medium.<sup>44</sup> Abdurakhmanov *et al.*<sup>116</sup> have made similar assumptions, asserting that the NBO coordinates Cu ions in BGs and that their influence is visible through the agglutination effect, which is the process by which alkali ions achieve electroneutrality.<sup>112,116</sup> However, a different study by Schuhladen *et al.*<sup>117</sup> revealed that the copper added to the borate glass resulted in a lesser release of Ca and B and a marginally reduced release of the other elements. Furthermore, the results discussed above showed that the influence of Cu doping in borosilicate glass led to a more stable glass network connectivity and a lower ions release rate during the degradation process. Again, this was because the Cu ions' agglutination effect and the agglomerate's charge balance in the glass network caused these effects.

Along with other ions found in BGs, the  $\text{Cu}^{2+}$  ion also has osteogenic capabilities that considerably enhance this property. Similarly, it has been demonstrated that Cu-doped BGs and scaffolds promote endothelial cell proliferation and increase

mesenchymal stem cell (MSC) differentiation levels.<sup>118,119</sup> To improve bone healing and anti-tumor therapy *via* the osteogenic properties of Cu, Libin *et al.*<sup>120</sup> recently doped BBG nanoparticles with Cu. According to an *in vitro* study, the nanoparticle increased endothelial cell angiogenesis as well as the differentiation potential of bone marrow stromal cells (BMSCs). Analyzing *in vivo*, restoring the severe bone abnormalities in rats was successfully possible.

More research revealed that the doped BG increased the expression of genes relevant to osteogenesis, including Runt-related transcription factor 2 (RUNX2), Collagen Type I Alpha 1 Chain (COL1A1), and Bone Morphogenetic Protein 2 (BMP2). This indicated that Cu-doped BBG could stimulate osteogenesis. Furthermore, through up-regulating the expression of the relevant osteogenic genes, Cu ions doped with BBG, according to certain additional studies, have been demonstrated to have a considerable impact on the process of secreting Vascular endothelial growth factors (VEGF). Thereby, through a multitude of growth factors, mediating angiogenesis in a multistep, complicated process.<sup>44,121</sup> On the other hand, concentration might be a factor in how Cu ions affect tissue regeneration. For example, in BG doped with 2.0 wt% CuO, Lin *et al.*<sup>122</sup> found that bone regeneration was improved along with blood vessels and fibrous tissue; however, the 0.4 and 0.8 wt% groups did not exhibit much angiogenesis in the neo-bone. Consequently, adding Cu to BBGs can endow the glass with outstanding angiogenesis while fostering bone repair and regeneration due to Cu's pro-osteogenic and pro-angiogenic qualities.

#### 4.2. Aluminium

In the presence of high amounts of Al<sub>2</sub>O<sub>3</sub>, it has been discovered that BBG exhibits noticeable bioactivity. According to NMR research, the quantity of aluminium ions in the glass matrix determines whether the ions are found in tetrahedral (AlO<sub>4</sub>) or octahedral (AlO<sub>6</sub>) structural units in borosilicate glass networks. It is anticipated that SiO<sub>4</sub> and BO<sub>4</sub> structural units will alternate with AlO<sub>4</sub> structural units, preventing the breakdown of the BGs structure.<sup>123</sup> Zhao *et al.*<sup>45</sup> conducted research on the impact of substituting varied quantities (0–2.5% mol.) of Al<sub>2</sub>O<sub>3</sub> for B<sub>2</sub>O<sub>3</sub> on the conversion of a borate glass to HAP in an aqueous phosphate solution. According to the study's results, BBG without Al<sub>2</sub>O<sub>3</sub> demonstrated the quickest reaction kinetics, with weight reduction reaching the highest level in only 3–4 days. Likewise, replacing 0.5 and 1.5 mol% B<sub>2</sub>O<sub>3</sub> in the initial glass with the equal mol% of Al<sub>2</sub>O<sub>3</sub> led to a reduction in weight reduction kinetics, with the glass components fully transforming to HAP by 9 and 12 days. In addition, the glass sample that had 2.5 mol% Al<sub>2</sub>O<sub>3</sub> in place of B<sub>2</sub>O<sub>3</sub> demonstrated a significantly delayed conversion rate to HAP, exhibiting weight reduction kinetics that, despite 30 days of reaction, approached roughly 70% of the highest value. Suggesting that Al<sub>2</sub>O<sub>3</sub> could drastically reduce the bioactivity of borate glass.

The weight loss of the glass and the change in the pH value of the solution slowed down as the glass' Al<sub>2</sub>O<sub>3</sub> content increased. This is because AlO<sub>4</sub> units in the glass limit how easily B<sup>3+</sup> and Na<sup>+</sup> ions can dissolve from the glass. After some

Na<sup>+</sup> and BO<sub>3</sub><sup>3-</sup> ion dissolution occurs during the conversion of the glasses, a porous Al-rich layer with AlO<sub>4</sub> units is produced on the glass' surface. This means that any Ca<sup>2+</sup> ions that dissolve from the glass must move *via* the Al-rich layer to interact with the PO<sub>4</sub><sup>3-</sup> in the solution to induce HAP deposition. Given that the structure of the AlO<sub>4</sub> units in the glass network is comparable to that of SiO<sub>4</sub>, the structure of the Al-rich layer is comparable to the Si-rich layer identified by Hench *et al.* for the transformation of silicate 45S5 glass.<sup>124</sup> As a result, the Al-rich layer's inhibitory effects on the solubility and permeability of ions from the glass likely caused the declines in the conversion rate of the glass composition.

Furthermore, because the AlO<sub>4</sub> units are negatively charged, they need to be synchronized to cations to preserve the structure's charge neutrality. Due to this, several of the Na<sup>+</sup> and Ca<sup>2+</sup> ions released from glass would become trapped in the porous Al-rich layer, inhibiting the interaction involving Ca<sup>2+</sup> and PO<sub>4</sub><sup>3-</sup> to deposit more HAP.<sup>45</sup> In short, the conversion rate of the glass reduces dramatically as the number of B<sub>2</sub>O<sub>3</sub> replaced by Al<sub>2</sub>O<sub>3</sub> increases.

Additionally, incorporating Al<sub>2</sub>O<sub>3</sub> into BG functions as a network former, producing more oxygen atoms that bridge with BO<sub>3</sub> units, thereby enhancing the material's long-term resilience, crack resistance, and chemical durability.<sup>125–127</sup> Even though adding a varying proportion of Al mol% in the BG composition can result in delayed HAP generation and other structural and chemical modifications, up to roughly 1.5 mol% Al<sub>2</sub>O<sub>3</sub> can be introduced into the glass composition without significantly reducing bioactivity.<sup>128</sup> Besides this, an experimental investigation by Mohini *et al.* demonstrates that the HAP occurrence of post-soaked Al-doped BBG sample gradually declines with an increase in Al<sub>2</sub>O<sub>3</sub> content up to 1.9 mol%, indicating a decrease in the glass's bioactivity.<sup>123</sup> Meanwhile, numerous investigations on the impact of Al-doped BBGs on their physicochemical and mechanical properties have been conducted.<sup>121,123–125,127–133</sup> Besides, a great deal of research has been done on the biological effects of aluminium, which is used in glass ionomers for dental cement and is known to be potentially toxic and to negatively influence biominerilization.<sup>134–138</sup> However, a thorough review of the literature reveals that studies on Al-doped BBGs, particularly their effect on critical osteogenic biomarkers and cell differentiation for bone regeneration, are still lacking.

#### 4.3. Strontium

The favorable effects of strontium-containing BGs on bone metabolism, reducing bone resorption, and increasing new tissue formation have recently piqued the interest of academics and scientists, both *in vitro* and *in vivo* studies.<sup>139,140</sup> Moreover, strontium ranelate, a daily oral prescription for osteoporosis treatment, has recently become recommended.<sup>141</sup> According to research, adding strontium has been shown to lower the dissolution of borate glass, resulting in a lower reaction mechanism of boron release. Such behavior, in particular, can be credited to the strontium ion's larger atomic radius of 2.15 Å when contrasted to Mg<sup>2+</sup> or Ca<sup>2+</sup> ions, with 1.6 Å and 1.97 Å

respectively; as such, larger radius ions require more space in the glass matrix, which is likely to limit the movement and discharge of the other ions, significantly lowering the dissolution rate of borate glass and potentially improving the glass network's bioactivity.<sup>142</sup> Yin *et al.*<sup>143</sup> developed BG scaffolds based on strontium-doped borate for bone tissue engineering (BTE). As per their findings, the presence of strontium in glass has no discernible influence on the structure. More specifically, increasing the strontium concentration within the borate-based glass network amplified the release of  $\text{Si}^{4+}$  and  $\text{Ca}^{2+}$  ions while significantly reducing the release of  $\text{B}^{3+}$  ions, suggesting that when the BG is soaked in SBF for *in vitro* bioactivity, BBG doped with a certain amount of strontium inhibits the rapid release of boron. Aside from controlling boron degradation and converting the glass surface to a nanosized hydroxyapatite layer in SBF, the influence of strontium ions within those scaffolds had a remarkable capacity to support MG-63 cells proliferation while also reducing the glass scaffolds' cytotoxicity.<sup>143</sup> In another study, Pan *et al.*<sup>144</sup> discovered that incorporating strontium into a borate glass matrix could not only regulate the rapid release of boron ions but also trigger the adherence of osteoblast-like cells, significantly boosting the cytocompatibility of borate glass. Furthermore, the production of multilayers of mineral phase with a porous structure suggests that complete breakdown is likely, as well as the proliferation of osteoblast cells overlaid by a new apatite film to create a layered structure may stimulate bone-like tissue synthesis earlier in the process. As a result, such innovative strontium-incorporated borosilicate Sr-BBG may function as a new breed of biomaterial for bone regeneration, delivering strontium to encourage the development of new bones while simultaneously providing boron as a nutritional element for bone health.<sup>144</sup>

Conversely, Sr has been shown to prevent bone loss and encourage bone regeneration. To completely comprehend how strontium facilitates bone regeneration by stimulating osteoblastic activity and suppressing osteoclastic resorption simultaneously, it is crucial to examine the biological response of strontium to BG compositions.<sup>145,146</sup> By examining the impacts of Sr on the physicochemical characteristics and osteogenic effectiveness of a bone cement made of BBG and a chitosan matrix, Xu *et al.*<sup>147</sup> could better understand the underlying molecular process that promotes bone regeneration. *In vitro* testing revealed that Sr substituted BBG cements increased expression of the osteogenic-related genes RUNX2, BSP, and OCN at 7, 14, and 21 days, respectively, with the highest significant increase being seen in the BBG cement with 6 mol% Sr. Furthermore, the cement's ability to promote cell proliferation and function *in vitro* and to mend bone lesions *in vivo* was improved at all levels of Sr substitution (0–12 mol% SrO) utilized in the study. Consequently, the creation of a HAP (or HA-type) product was slowed down when Sr was substituted. Interestingly, the outcomes of Xu *et al.*'s investigation are comparable to those of another study that found that Sr had a stimulating influence on the activity of osteoblastic cells.<sup>148,149</sup> Results also showed that Sr inclusion up to 12 mol% (see Fig. 7) in BG composition had no cytotoxic properties.<sup>144</sup>

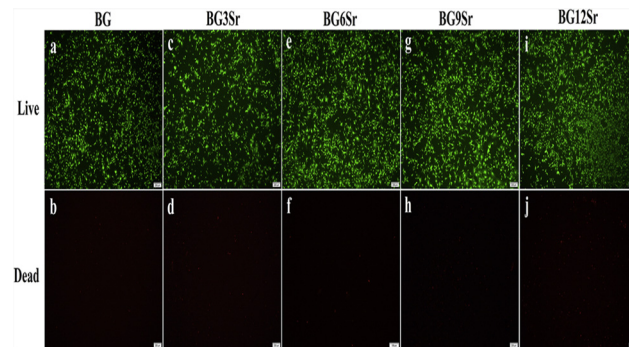


Fig. 7 Live–dead assay to evaluate the cytotoxicity of Sr doped BBG cement extracts to hBMSCs.<sup>147</sup> licensed under a Creative Commons Attribution Non-Commercial-No Derivatives 4.0 International (CC BY-NC-ND 4.0) (<https://creativecommons.org/licenses/by-nc-nd/4.0/>).

The pathway through which Sr promotes osteogenic gene expression in MSCs (mesenchymal stem cells), alkaline phosphatase activity (ALP), and osteoprotegerin (OPG) secretion in osteoblasts can be conceptualized as OPG expression in osteoblasts that inhibits the relationship between RANK (receptor activator of nuclear factor-B) and its ligand (RANKL, receptor Activator of Nuclear Factor-B Ligand), thereby preventing osteoclastogenesis. Similarly, it has been discovered that Sr increases the production of angiogenic factors, causing a link between angiogenesis and osteogenesis.<sup>150–152</sup>

Although, in bone regenerative therapies, enhancing and expediting bone recovery are still unmet needs, strontium-doped BGs are auspicious materials to address this issue. However, various borate-based BGs doped with strontium and manufactured in multiple forms have now been created and characterized for treating bone deformities and injuries.<sup>140,144,153–159</sup>

#### 4.4. Titanium

Materials containing titanium ( $\text{Ti}^{4+}$ ) have been employed extensively in medical applications because of the metal's related bioactivity *in vivo*. Similarly, studies have demonstrated that titanium dioxide ( $\text{TiO}_2$ ) with a concentration lower than 10 ppm is cytocompatible and has no appreciable impact on cell viability. When in contact with bodily fluids, it also promotes the formation of HAP and increases osteoblast differentiation. Previous research has suggested that increasing the proportion of  $\text{TiO}_2$  in glass can alter its function as a network-forming or network-modifying oxide, which will subsequently affect its solubility and make it easier to adjust the degradation process.<sup>78,160–165</sup> One of the study goals in previous work by Romina *et al.*<sup>166</sup> was to evaluate the dissolution rate and the ion release effects of  $\text{TiO}_2$  incorporation on the morphology of BBG scaffolds. They suggest that the chemical structure of the samples, rather than the wall thickness influence, is the possible source of the ion release effects. As a result, an increase in  $\text{TiO}_2$  content induces the modification of  $\text{BO}_3^{3-}$  with  $\text{Ti}^{4+}$  in the B–O–B bond, resulting in the formation of the B–O–Ti structure. More so,  $\text{TiO}_2$  ions having a modest atomic

radius of 1.47 Å and a big electric charge improves network connectivity which may explain why the combined ion dissolution rate of scaffolds decreases with increasing Ti<sup>4+</sup> composition. The ion release and pH results reported in this research show that by introducing TiO<sub>2</sub> into the glass network of the scaffolds, the dissolution rate of borate-based BG can be controlled.<sup>166,167</sup> According to the findings of this research, Ti-doped BBGs scaffolds could be a viable option for treating bone loss during revision total knee arthroplasty (rTKAs). In another work by Omar *et al.*, it was discovered that BBGs with 0 and 15 mol percent of titanium dioxide added had much better antibacterial activities and higher solubility than their silica-based equivalents. Conversely, because there is a lack of study in this area, *in vivo* studies would be necessary to assess the impact of a dynamic environment on osteogenic cell markers and tissue response to Ti-doped BBGs.

## 5. Applications of BBGs

Widespread usage of BGs in biomedical and healthcare applications, as indicated in Fig. 8, has opened the way for contemporary biomaterial-driven regenerative medicine that primarily repairs bone<sup>109,168,169</sup> and dental anomalies,<sup>170</sup> in addition to wound healing.<sup>171</sup> This is because when an implant is placed in a biological environment, a sequence of events creates an apatite layer, which then causes the tissue to bind. Additionally, BG has been demonstrated to promote neocartilage production during the *in vitro* cultivation of chondrocyte-seeded hydrogels and to act as a subchondral framework for tissue-engineered osteochondral structures.<sup>105</sup> Finally, since BBGs can adhere to the bone and even soft tissues, they have found relevance in biomedical applications (see Table 2).

### 5.1. Wound care

By using a three percent boric acid solution to deep scars, boron has substantially revamped wound healing since 1990, cutting the time necessary in critical care by two-thirds. Besides

acting on the extracellular environment, the boric acid solution increased the healing of wounds, according to an *in vitro* study on human fibroblasts.<sup>172</sup> Further *in vitro* research demonstrated that these potential benefits of boron were brought on by its direct interactions with some fibroblast enzymes, notably elastase, trypsin-like enzymes, collagenase, and alkaline phosphatase. These results suggest that boron is essential for wound healing and helps fibroblasts' important enzymes function, which enhances extracellular matrix renewal.<sup>58,172–177</sup> Boron's ability to treat deep wounds and chronic diabetic foot ulcers has led to its use as a network former in BBGs, a relatively new development in the field of wound management. Even though the United States Food and Drug Administration (FDA) endorsed the first BG for medicinal use in 1985, a wound management product containing BBG (13-93B3) did not receive FDA approval until 2016.<sup>178,179</sup> Demonstrating the importance of conducting additional research on this type of BG has significantly lowered attention from scientists and researchers.<sup>30,180</sup>

A novel borate-based bioactive glass fiber (BBGF) for the treatment of acute and chronic wounds was evaluated for effectiveness and relevance by Donald (2020). Four patients with persistent wounds who had failed various past sophisticated therapies and procedures were treated with MIRRAGEN, a commercialized product made of 13-93B3 glass microfibers. Compared to the average wound duration of 391 days, the results of this treatment with BBGF revealed that all patients experienced effective wound closure in an average of only 55 days. In addition to promoting faster healing and better patient outcomes, BBGF significantly improves the healthcare system by lowering the cost of treating chronic wounds, which was previously estimated to be \$87 750 per patient, to an average of \$3 564 per patient.<sup>181</sup> In another study, researchers from several institutes conducted a comparable randomized two-parallel group trial to learn more about the efficacy of MIRRAGEN as a treatment for persistent diabetic foot ulcers compared with the standard of care treatment. After randomization, individuals received treatment for 12 weeks, with the outcome measure being the likelihood of fully healed wounds. Following this therapy time, wound examination revealed that 70% of the MIRRAGEN-treated ulcers had recovered, relative to 25% of those treated solely with standard-of-care (SOC).

Additionally, compared to the SOC group, the average percentage surface decline for the wounds treated with MIRRAGEN was 79% instead of 37%. Contrary to the SOC group, the MIRRAGEN group experienced no ulcer-related infections.<sup>178</sup> These outcomes of infection control measures can be thought to be due to the antibacterial potential of boron in the BG structure, as boron ions alone have been shown to prevent the development of both Gram-positive and Gram-negative bacteria by disrupting the integrity of bacteria's cell membranes, as well as, by suppressing the growth of biofilms.<sup>182,183</sup>

In addition to effectively treating chronic wounds, BBGs can also be electrospun to form a fibrous structure similar to the extracellular matrix of the skin tissue for a wound dressing. For instance, Schuhladen *et al.*<sup>184</sup> created a fiber mat utilizing methylcellulose and poly(-caprolactone). More so, Manuka

Borate based BG	Properties	Applications
Sol-gel derived	Angiogenesis	Osteoporosis
Melt derived	Osteogenesis	Wound healing
Scaffolds	Antibacterial	Bone implant coating Dental implant coating

Fig. 8 Techniques, properties, and biomedical applications of bioactive borate glass.

Table 2 General overview of different medical applications of doped BBGs

Title	Type of BG	Bone regeneration applications	Remarks	Ref.
Evaluation of borate bioactive glass scaffolds as a controlled delivery system for copper ions in stimulating osteogenesis and angiogenesis in bone healing	MQ BBG	Bone healing	Controlled delivery of copper (Cu) ions from borate bioactive glass scaffolds for stimulating angiogenesis and osteogenesis in a rodent calvarial defect model was investigated. Scaffolds doped with 3 wt% CuO showed a significantly better capacity to stimulate angiogenesis and regenerate bone when compared to the undoped glass scaffold.	43
Bioactive borate glass scaffolds: <i>in vitro</i> and <i>in vivo</i> evaluation for use as a drug delivery system in the treatment of bone infection	MQ BBG	Bone infection treatment	BG scaffolds loaded with the drug were implanted into the right tibiae of rabbits infected with osteomyelitis. HAP formed <i>in vivo</i> , served as a structure to support the growth of new bone and blood vessels	109
Osteogenic and anti-tumor Cu and Mn-doped borosilicate nanoparticles for synergistic bone repair and chemo dynamic therapy in bone tumor treatment	SG BBG	Bone repair and tumor treatment	Cu and Mn-doped borosilicate nanoparticles (BSNs) were developed for synergistic bone repair and anti-tumor treatment. <i>In vitro</i> study showed that BSNs promoted both osteogenic differentiation of BMSCs and angiogenesis of endothelial cells and consistently, the critical bone defects of rats were efficiently repaired by BSNs through <i>in vivo</i> evaluation.	120
Mesoporous bioactive glass-coated 3D printed borosilicate bioactive glass scaffolds for improving repair of bone defects	3D printed BBG scaffold	Bone healing	3-D scaffolds with mesoporous BBG were fabricated by the 3D printing technique. Biocompatibility of the BG-MBG scaffolds was evaluated by assessing biodegradability, cell proliferation, and alkaline phosphatase (ALP) activity of osteogenic gene expression with human bone marrow stromal cells (hBMSCs). Results showed that the scaffolds possess good biodegradability and stimulated the proliferation and osteogenic differentiation of hBMSCs. <i>In vivo</i> studies showed that the BG-MBG scaffolds could significantly enhance new bone formation in both inner and peripheral scaffolds in defects.	217
Synthesis and characterization of sol-gel bioactive glass nanoparticles doped with boron and copper	SG BBG	Prior investigation for use as an angiogenic biomaterial in soft TE	The BG nanoparticles can be considered novel promising angiogenic and antibacterial agents and have interesting potential applications in the soft TE field	218
Novel strontium borate modified Hench's bioglass synthesis and characterization for bone replacement	MQ BBG	Bone replacement	The effect of strontium on the BGs' structural and biological behavior was investigated. Glass powders were immersed in a simulated fluid body (SBF) solution over varied periods, 1, 2, 3, and 4 weeks, to investigate the bioactivity of prepared samples. Results showed that Sr promotes the formation process of crystalline hydroxyapatite. Thus, it could be one of the best materials for bone regeneration application.	219
Investigation of the influence of SrO addition on the bioactivity of CaO-Na <sub>2</sub> O-P <sub>2</sub> O <sub>5</sub> -B <sub>2</sub> O <sub>3</sub> glass system	MQ BBG	Bone tissue growth	The role of strontium oxide in the BGs calcium-sodium-borate was studied to evaluate the bioactivity of the system and the rate of the ion release in SBF. Results show that SrO-doped calcium-sodium-borate glasses are materials with a high rate of bioactivity, low cytotoxicity, and reduced dissolution rate of the glasses in an aqueous medium; besides, they induce cell proliferation and bone tissue growth with living tissues.	220
<i>In vivo</i> bioactivity assessment of strontium-containing soda-lime-borate glass implanted in femoral defect of rat	MQ BBG	Bone regeneration	<i>In vivo</i> bioactivity assessment of strontium-doped borate glass implanted in rat femoral defect was carried out. <i>In vivo</i> bioactivity test showed that implantation of all borate glasses did not demonstrate local or general complications in all rats, and they exhibited nearly complete bone mineralization.	221
Evaluation of novel injectable strontium-containing borate bioactive glass cement with enhanced osteogenic capacity in a critical-sized rabbit femoral condyle defect model	MQ BBG	Bone regeneration	Strontium-doped borate bioactive glass particles and a chitosan-based bonding phase were prepared and evaluated <i>in vitro</i> and <i>in vivo</i> . Compared to borate glass particles without Sr,	155

Table 2 (continued)

Title	Type of BG	Bone regeneration applications	Remarks	Ref.
Effects of strontium-doped bioactive glass on the differentiation of cultured osteogenic cells	SG BBG	Bone cell behavior	the Sr-BBG cement enhanced the proliferation and osteogenic differentiation of hBMSCs <i>in vitro</i> . The Sr-BBG cement showed a better capacity than the BBG cement to regenerate bone at the implant–bone interface at 4- and 8-weeks post-implantation in a critical-sized rabbit femoral condyle defect model	222
Mechanistic study of the bioactivity improvement of $\text{Al}_2\text{O}_3$ -doped BBG after dynamic flow treatment	MQ BBG	Bone cell differentiation	<i>In vitro</i> effect of a new Sr-doped bioactive glass manufactured by the sol-gel method on osteoblast viability and differentiation. Osteoblast differentiation of fetal mouse calvarial cells was enhanced in the presence of bioactive glass particles containing 5 wt% strontium. The effect of dynamic flow treatment on the biological properties of $\text{Al}_2\text{O}_3$ -doped BBG was investigated. Results revealed that the SBF-treated $\text{Al}_2\text{O}_3$ -doped BBG exhibits a significantly reduced degradation rate and improved bioactivity. <i>In vitro</i> cell studies suggested that the $\text{Al}_2\text{O}_3$ -doped BBG, after being treated by dynamic flow treatment, boosts the proliferation of MC-3T3E1 cell	223
Title	Type of BG	Wound healing applications	Remarks	Ref.
Angiogenesis and full-thickness wound healing efficiency of a copper-doped borate bioactive glass/poly (lactic- <i>co</i> -glycolic acid) dressing loaded with vitamin E <i>in vivo</i> and <i>in vitro</i>	MQ BBG	Wound healing	Cu-doped borate bioactive glass/poly(lactic- <i>co</i> -glycolic acid) loaded with vitamin E (0-3.0 wt% vitamin E) was fabricated to evaluate its efficiency for angiogenesis in cells and full-thickness skin wounds healing in rodents. Results indicated that the Cu-doped biomaterial loaded with vitamin E is effective in stimulating angiogenesis and healing full-thickness skin defects	224
Wound dressings composed of copper-doped borate bioactive glass microfibers stimulate angiogenesis and heal full-thickness skin defects in a rodent model	MQ BBG	Wound dressing	Results showed that the ionic dissolution product of the biomaterial was not toxic to HUVECs and fibroblasts, promoted HUVEC migration, and secretion of VEGF, as well as stimulating the expression of angiogenic-related genes of the fibroblasts. These results indicate that the Cu-doped borate glass microfibers have a promising capacity to stimulate angiogenesis and heal full-thickness skin defects	121
<i>In vitro</i> study of improved wound-healing effect of bioactive borate-based glass nano-/micro-fibers	BBG & SIG	Wound healing	Comprehensive material analysis and biocompatibility evaluation of a silicate-based (45S5) and two borate-based (13-93B3 and 1605) nano-/micro-scale bioactive glass fibers were carried out. Evaluation on human skin cell line demonstrated that in comparison with silicate-based fibers, borate-based fibers, under static condition, can significantly stimulate cell growth with higher cell proliferation rate. Moreover, the trace amount doping of metal species within the glass composition, such as copper and zinc, are also potentially important in glass conversion, biocompatibility as well as bioactivity.	225
<i>In vivo</i> and <i>in vitro</i> studies of borate-based glass microfibers for dermal repairing	MQ BBG & SIG	Wound healing	BBG micro-fibers were fabricated and compared with the traditional 45S5 Bioglass® micro-fibers. The BBG micro-fiber wound dressings enhanced the formation of blood vessel, and resulted in a much faster wound size reduction than the SiG micro-fibers, and also than the control groups, after 9 days application.	226
<i>In situ</i> forming hydrogel based on thiolated chitosan/carboxymethyl cellulose (CMC) containing borate bioactive glass for wound healing	MQ BBG	Wound healing	Thiolated chitosan (tCh)/oxidized carboxymethyl cellulose (OCMC) hydrogel containing Cu-doped borate bioglass (BG) was developed as a wound dressing to improve wound healing in a full-thickness skin defect of mouse animal model. Investigations revealed that	227

Table 2 (continued)

Title	Type of BG	Wound healing applications	Remarks	Ref.
			the hydrogel containing borate BG had potential enough for wound occlusion <i>in vivo</i> and elevated blood vessel formation throughout the wound repair procedure.	
Title	Type of BG	Dental and implant coating applications	Remarks	Ref.
Bioactive borate glass coatings for titanium alloys	MQ BBG	Implant coating	BBG coatings was developed for titanium and titanium alloys. The glasses convert to bioactive hydroxyapatite coatings when exposed to simulated body fluid. Also, assays with MC3T3-E1 pre-osteoblastic cells show the borate glasses exhibit <i>in vitro</i> biocompatibility	97
Borate and silicate bioactive glass coatings prepared by nanosecond pulsed laser deposition	MQ BBG &SIB	Implant coating	Silicate (13-93) and borate (13-93-B3) bioactive glass coatings were deposited on titanium using the nanosecond Pulsed Laser Deposition technique. Cytocompatibility and osteogenic differentiation tests showed that thin films retain the biocompatibility properties of the target silicate and borate glass, respectively. However, no antibacterial activity of the borate glass films was observed, suggesting that ion doping is advisable to inhibit bacterial growth on the surface of borate glass thin film	228
Borate modified bioglass containing scaffolds for dental tissue engineering applications	SG BBG	Dental TE	The effects of BBG on the odontogenic differentiation of human dental pulp stem cells (hDPSCs) were investigated. All BG groups enhanced odontogenic differentiation of hDPSCs and the presence of borate increased cell viability. Immunohistochemical and histochemical stainings showed that scaffolds positively affected the odontoblastic differentiation of the hDPSCs.	229

honey, unique honey made from the indigenous New Zealand tree *Leptospermum scoparium*,<sup>185</sup> was used to cross-link these fiber mats, which were employed as a biodegradable delivery system for BBG particles. Incorporating BBG into the fiber mats enhanced their bioactivity, according to the team's degradation experiments using simulated bodily fluid. Similarly, cellular biology investigations using human dermal fibroblasts and cells comparable to keratinocytes in humans demonstrated the great potential of the manufactured composite fiber mats as a material for wound dressing, mainly due to their capacity to support wound closure that is typically attributed to the presence of BBG.<sup>184</sup> A unique Nano-sized carbonated hydroxyapatite (HCA) covered with BBG was another intriguing approach Chen *et al.*<sup>103</sup> reported to assess its influence on mouse models for wound repair. By dynamically submerging the BBG particles in a flowing buffer medium, Nano-HCA was neo-formed.

In addition to increasing the biocompatibility and maintaining the biodegradability of the BBG, the porous structure was a little more surface-coated with a layer of amorphous HCA. Nano-HCA BBG on wound healing were then assessed and contrasted to those of the Nano-HCA and 45S5® at the *in vitro* and animal levels. The research's findings showed no negative surgical outcomes and that the proportion of wound scars decreased in all 5 groups. Specifically, wounds administered with Nano-HCA BBG particles virtually entirely healed rapidly during the seventh day (98%), in contrast to wounds left untreated (60%). Additionally, Nano-HA and 45S5® had a somewhat substantial impact on wound healing, as evidenced by the fact that their wound healing rates (61% and 63%,

respectively) were essentially in the same range as those of the control group. As a result, the wound healing efficiency of the Nano-HCA BBG group enhances biocompatibility, encourages cell growth, and aids in wound healing in rodent skin deficiencies. Another recent finding on the need for a better wound dressing that possesses the angiogenic capacity for rapid healing of full-thickness skin wounds was developed by Shichang *et al.*<sup>121</sup> In their investigation, copper-doped BBG microfiber materials were developed and tested both *in vivo* and *in vitro*. The fibers decayed and changed into hydroxyapatite after being submerged in simulated bodily fluid for around 7 days.

Similarly, *in vitro* cell culture demonstrated that the fibers' ionic dissolving product was not hazardous to fibroblasts and human umbilical vein endothelial cells (HUVECs). Instead, it induces the expression of fibroblasts' angiogenic-related genes. At 7 and 14 days after surgery, when used to treat full-thickness skin defects in mice, Cu-doped fibers had a much higher effect of promoting revascularization than the undoped fibers and the untreated defects (control). Comparing the Cu-doped and undoped fiber-treated defects to the untreated defects, the treated defects demonstrated enhanced collagen deposition, maturity, and orientation. These findings indicate a promising ability of the Cu-doped borate glass microfibers to promote angiogenesis and repair full-thickness skin defects.

## 5.2. Bone tissue engineering

Common diseases like bone defects cause individuals to experience physical pain and can even make them disabled. Biomedical materials research is investigating and attempting

to tackle a significant issue: how to correct these faults by creating novel bone repair materials.<sup>105,186,187</sup> It is well recognized that boron, which seems frequently found in water and food in modest proportions, is crucial for the nutritional process of developing healthy bones in both humans and animals.<sup>188,189</sup> Borate levels in bone are also discovered to be noticeably greater than in other tissues in addition to swiftly dispersing across bodily fluids and still being eliminated *via* urination. According to reports, 99% of the boric acid from a single intravenous injection got eliminated unaltered in the urine for 120 hours, and no propensity for boron accumulation was seen.<sup>57,188–190</sup> These results indicate that more research into the possible use of borate glasses in bone healing and tissue engineering is necessary for bone health.

Moreover, chronic bone infections like osteomyelitis are typically accompanied by contamination of the surrounding tissues, poor perfusion, and bone necrosis. Because of this, only a small number of antibiotics given orally or intravenously can effectively treat an infection. Nevertheless, commercially accessible biomaterials, notably poly(methyl methacrylate; PMMA), have been employed in clinical situations as delivery systems for many years. However, once PMMA has finished functioning as a drug carrier, further procedure is needed to eliminate them from the body. Furthermore, polymers like collagen, poly(lactic acid), and polylactides cannot organically bond with bone despite being biodegradable. Nonetheless, inorganic materials such as calcium phosphate cement, hydroxyapatite (HAP), and BBG, including S53P4 with antimicrobial capabilities, tend to attach effectively to bone tissues and may also serve as a medication delivery mechanism for bone healing.<sup>89,191–197</sup>

Zhang *et al.*<sup>198</sup> conducted a study to show that BBG degrades more quickly and has pro-osteogenic effects than  $\beta$ -TCP, which could greatly enhance huge segmental bone defect healing. In brief, the potential of the BBGs to treat significant segmental bone lesions was assessed using a critical-sized rabbit radius defect model. The effect of BBGs on bone marrow mesenchymal stem cells (BMSCs') osteogenic development was also evaluated. Investigations were also conducted into how the BBGs solubility by-products influenced the bone morphogenetic protein (BMP)/Smad signal pathway activity in BMSCs. *In vitro* findings show, BBG has better bone regeneration benefits than  $\beta$ -TCP. The analysis also indicates that BBG dissolution products considerably enhance BMSCs' osteogenic development, resulting in the repair and regeneration of bone defects. As a result, the BBG used in this work can be a potential and good bone tissue regeneration material with a wide range of possible applications. The ability of BBG (1393B3 and Cu-doped 13-93B3) to regenerate bone in a rat calvarial defect model was examined in another study by Lianxiang *et al.*<sup>199</sup> They examined the impact of three different microstructures (trabecular, oriented, and fibrous) on this capacity. Histomorphometric analysis and scanning electron microscopy (SEM) was used to monitor the scaffolds for 12 weeks to measure the quantity of new bone growth, mineralization, and blood vessel area. They showed that for the trabecular, oriented, and fibrous

microstructures, new bone formed in proportions of 33%, 23%, and 15%, respectively, to the overall defect area. According to subsequent comparisons made by the team, 19% of new bone was generated in implants made of silicate 45S5 BG particles. However, doping the borate glass with 0.4 wt% copper (CuO) had minimal impact on bone regeneration in trabecular and oriented scaffolds. It considerably positively impacted bone regeneration in the fibrous scaffolds, increasing it from 15 to 33 percent. Moreover, blood vessels penetrated all scaffolds, with the average blood vessel area being larger in trabecular scaffolds than in oriented and fibrous scaffolds. According to the team's research, all three scaffold microstructures successfully supported bone regeneration, although the trabecular scaffolds supported more bone growth and may hold the most promise for bone tissue regeneration.

Numerous cell sources have been studied for bone regeneration using doped BBGs, including bone marrow mesenchymal stem/progenitor cells, osteoblasts, cells genetically engineered to express osteogenic factors, embryonic stem cells, and others. Conversely, various studies have indicated that distinct bone growth factors, such as bone morphogenetic protein (BMP), serve essential roles in the progression of bone regeneration, making a significant difference in the differentiation of osteogenic progenitor cells into osteoblasts and the mineralization of bone (see Table 2). Furthermore, new bone repair materials which include hydrogel, nanofiber scaffolds, and 3d-printed scaffolds are being developed.<sup>5,200–203</sup> These translational approaches to bone healing based on engineering cells and biomaterial scaffolds promise to impact the future of bone tissue engineering.

### 5.3. Bone and dental implant coatings

Because BGs can form a strong bond with a living person's bone tissues, they are widely employed in dental and orthopedic implants.<sup>204,205</sup> However, their weak mechanical characteristics, particularly their brittleness, are mainly used as coatings over mechanically resilient substrates, such as titanium, alumina, and zirconia. Surface coating is a common and extensively used technique to increase biomaterials' surface bioactivity and biocompatibility. Compared to other metallic materials, BGs are remarkably biocompatible and have a higher probability of integrating into human tissue than the metal implants mentioned earlier. Because of this, BG is an excellent choice for strengthening the biocompatibility and bioactivity of these metals, enhancing the substrates' mechanical characteristics, and providing antibacterial capabilities *via* the slow release of therapeutic ions. As a result, BGs are widely used in orthopedic, spinal, craniomaxillofacial, and periodontal applications.<sup>206–211</sup>

Antibacterial effects of sodium borate and calcium borate-based polymeric coatings for orthopedic implants were recently reported by Huseyin *et al.*<sup>212</sup> Their goal was to compare the antibacterial and biofilm-degrading characteristics of titanium implants coated with sodium borate and calcium borate minerals to implants without coating and implants coated with alginate. The team discovered that the implant coated with

alginate had the highest bacteria load, while biofilm development was also found on the implant without coating. Although, at a low concentration of borate minerals, scaffolds had lower microbial loads than implants without coating. But at high concentrations of  $0.5 \text{ mg mL}^{-1}$  and  $0.75 \text{ mg mL}^{-1}$ , borate minerals showed a potent antibacterial effect on colonization and biofilm formation on the implant surface.<sup>212</sup> In further pertinent work, Teicoplanin-loaded BBG implants for treating chronic bone infection in a rabbit tibia osteomyelitis model were investigated by Xin *et al.*<sup>213</sup> Within 12 weeks of being implanted in a rabbit tibia, pellets made of a combination of teicoplanin powder and BBG particles were able to heal a chronic bone infection. Over about 9 days *in vivo*, the pellets delivered a consistent release of teicoplanin. Furthermore, the BG particles simultaneously broke down in the bodily fluid and transformed into porous HA-type grafts that encouraged the new bone formation and solidly adhered to the neoformed bone, healing the bone defect.

On the other hand, BGs have also been employed clinically in creating dental recovery materials that can remineralize after microbial infections. The BG nanoparticles hasten the production of new bone, which stops gingival and epithelial cells from migrating down the tooth. As such, it is possible to stabilize the junction created between the tooth and the periodontal membrane.<sup>207,214</sup> Additionally, BG particles have been utilized in mouthwashes to address oversensitive teeth. These BG particles are believed to adhere to the dentine, so the local pH rises due to released ions. This also causes HCA to precipitate over the tubule end, shielding the tubules from exposure to liquid flow.<sup>214–216</sup>

## 6. Conclusion and future outlook

Over the past 50 years, significant effort has been made in the biomedical field to develop BGs, notably those with a 45S5 composition. This created an approach for creating glasses with borate compositions, bringing about new prospects for using BBGs in tissue engineering. Because of their biodegradable properties, as well as doping with several metallic ions, BBGs have shown their ability to support osteogenesis. Likewise, recent work has also demonstrated its angiogenic potential, which may benefit soft tissue repair. In addition, doped BBGs have proved to be effective in promoting osteogenic biomarkers such as BMP, OPG, RUNX2, RANK/L, BSP, *etc.* Consequently, these BGs have been shown to activate angiogenic growth factors such as VEGF, thus providing unique opportunities for the target delivery of therapeutic ions for wound healing. Furthermore, despite its brittleness, BBG possesses distinct features that include the ability to possess CTE closer to the bio-metallic substrate, thereby resulting in a better performance at coating the substrate interface than their silica-based glasses equivalents.

The current literature has clearly shown that doped BBGs can enhance the physico-chemical properties of the glass system as well as stimulate angiogenesis and upregulate key

osteogenic biomarkers, which are useful in soft and hard tissue regeneration. However, despite the academic community's curiosity, there is still a lack of understanding of how Al/Ti-doped BBGs affect critical osteogenic biomarkers and cell differentiation for bone regeneration. Conversely, literature has shown that very few previous studies have investigated the synthesis of BBGs using the sol-gel technique. Another area that has been less exploited is additive manufacturing to prepare BBGs scaffolds. In light of these limitations and to support their use in biomedical applications, there is a need for further detailed *in vitro* and *in vivo* studies that would be necessary to assess the impact of a dynamic environment on osteogenic cell markers and tissue response to Al/Ti-doped BBGs. Furthermore, researchers must focus on utilizing the sol-gel technique in synthesizing BBGs due to the potential advantages (greater porosity and bioactivity) over the melt-quench method. Similarly, there is a need to expand 3D printing to prepare BBGs scaffolds.

Summarily, this review presents a general overview of the borate-based BG systems, emphasizing their composition, properties, and uses for bone regeneration, wound healing, and coatings for dental and bone implants. The main focus is on the role of doping ions in regulating the degradation process of BBGs and their effects on osteogenic biomarkers that regulate the process of bone healing.

## Abbreviations

Al	Aluminium
ALP	Alkaline phosphatase activity
BGs	Bioactive glasses
BBG	Borate bioactive glass
BBGF	Borate-based bioactive glass fiber
BMP	Bone morphogenetic protein
BMSCs	Bone marrow mesenchymal stem cells
BTE	Bone tissue engineering
COL1A1	Collagen type 1 alpha 1
CTE	Coefficient of thermal expansion
Cu	Copper
FDA	Food and drug administration
HAP	Hydroxyapatite
HUVECs	Human umbilical vein endothelial cells
MQ BBG	Melt quench borate-based bioactive glass
NBO	Non-bridging oxygen
NMR	Nuclear magnetic resonance
OPG	Osteoprotegerin
PMMA	Poly methyl methacrylate
RUNX2	Runt-related transcription factor 2
SBF	Simulated body fluid
SEM	Scanning electron microscopy
SG BBG	Sol-gel borate-based bioactive glass
SOC	Standard of care
Sr	Strontium
T <sub>g</sub>	Glass transition temperature
Ti	Titanium
VEGF	Vascular endothelial growth factor

## Conflicts of interest

There is no conflict of interest to declare.

## Acknowledgements

The authors would like to acknowledge the Euro-Mediterranean University of Fes for their support.

## References

- 1 L. L. Hench, *J. Mater. Sci.: Mater. Med.*, 2006, **17**, 967–978.
- 2 L. L. Hench, R. J. Splinter, W. C. Allen and T. K. Greenlee, *J. Biomed. Mater. Res.*, 1971, **5**, 117–141.
- 3 J. Wilson, G. H. Pigott, F. J. Schoen and L. L. Hench, *J. Biomed. Mater. Res.*, 1981, **15**, 805–817.
- 4 E. A. Abou Neel, D. M. Pickup, S. P. Valappil, R. J. Newport and J. C. Knowles, *J. Mater. Chem.*, 2009, **19**, 690–701.
- 5 H. A. Awad, R. J. O’Keefe and J. J. Mao, *Bone Tissue Engineering*, INC, 2020.
- 6 H. A. Awad, R. J. O’Keefe, C. H. Lee and J. J. Mao, *Bone Tissue Engineering: Clinical Challenges and Emergent Advances in Orthopedic and Craniofacial Surgery*, Elsevier, 4th edn, 2013.
- 7 H. Qu, H. Fu, Z. Han and Y. Sun, *RSC Adv.*, 2019, **9**, 26252–26262.
- 8 A. Ibrahim, *3D bioprinting bone*, Elsevier Ltd, 2018.
- 9 S. A. Brigido, N. M. Protzman, M. M. Galli and S. T. Bleazey, *Foot Ankle Spec.*, 2014, **7**, 377–386.
- 10 G. Zimmermann and A. Moghaddam, *Injury*, 2011, **42**, S16–S21.
- 11 V. Campana, G. Milano, E. Pagano, M. Barba, C. Cicione, G. Salonna, W. Lattanzi and G. Logroscino, *J. Mater. Sci.: Mater. Med.*, 2014, **25**, 2445–2461.
- 12 R. Dimitriou, G. I. Mataliotakis, A. G. Angoules, N. K. Kanakaris and P. V. Giannoudis, *Injury*, 2011, **42**, S3–S15.
- 13 S. Ali, A. M. Abdul Rani, Z. Baig, S. W. Ahmed, G. Hussain, K. Subramaniam, S. Hastuty and T. V. V. L. N. Rao, *Corros. Rev.*, 2020, **38**, 381–402.
- 14 A. J. Sunija, *Biomaterials and biotechnological schemes utilizing TiO<sub>2</sub> nanotube arrays-A review*, Elsevier Ltd, 2018.
- 15 S. V. Bhat, *Overview of Biomaterials*, Springer, 2002, pp. 1–11.
- 16 F. Baino, M. Tomalino and D. Tulyaganov, *PoliTO Springer Series Ceramics, Glass and Glass-Ceramics From Early Manufacturing Steps Towards Modern Frontiers*, 2021.
- 17 G. Kaur, *Bioactive glasses-Potential Biomaterials for Future Therapy*, 2017.
- 18 X. Liu, H. Pan, H. Fu, Q. Fu, M. N. Rahaman and W. Huang, *Biomed. Mater.*, 2010, **5**, 015005.
- 19 X. Lu, J. Kolzow, R. R. Chen and J. Du, *Bioact. Mater.*, 2019, **4**, 207.
- 20 M. Bohner and J. Lemaitre, *Biomaterials*, 2009, **30**, 2175–2179.
- 21 A. A. Zadpoor, *Mater. Sci. Eng., C*, 2014, **35**, 134–143.
- 22 S. Fujibayashi, M. Neo, H. M. Kim, T. Kokubo and T. Nakamura, *Biomaterials*, 2003, **24**, 1349–1356.
- 23 E. Jablonská, D. Horkavcová, D. Rohanová and D. S. Brauer, *J. Mater. Chem. B*, 2020, **8**, 10941–10953.
- 24 T. H. Qazi, S. Hafeez, J. Schmidt, G. N. Duda, A. R. Boccaccini and E. Lippens, *J. Biomed. Mater. Res. A*, 2017, **105**, 2772.
- 25 F. Westhauser, F. Hohenbild, M. Arango-Ospina, S. I. Schmitz, S. Wilkesmann, L. Hupa, A. Moghaddam and A. R. Boccaccini, *Int. J. Mol. Sci.*, 2020, **21**, 1639.
- 26 A. Yao, D. Wang, W. Huang, Q. Fu, M. N. Rahaman and D. E. Day, *J. Am. Ceram. Soc.*, 2007, **90**, 303–306.
- 27 Q. Fu, M. N. Rahaman, B. Sonny Bal, R. F. Brown and D. E. Day, *Acta Biomater.*, 2008, **4**, 1854–1864.
- 28 Q. Fu, M. N. Rahaman, B. S. Bal, W. Huang and D. E. Day, *J. Biomed. Mater. Res. A*, 2007, **82**, 222–229.
- 29 S. Cavalu, F. Banica, C. Gruian, E. Vanea, G. Goller and V. Simon, *J. Mol. Struct.*, 2013, **1040**, 47–52.
- 30 W. Huang, D. E. Day, K. Kittiratanapiboon and M. N. Rahaman, *J. Mater. Sci.: Mater. Med.*, 2006, **17**, 583–596.
- 31 L. Moimas, M. Biasotto, R. Di Lenarda, A. Olivo and C. Schmid, *Acta Biomater.*, 2006, **2**, 191–199.
- 32 L. Xia, W. Ma, Y. Zhou, Z. Gui, A. Yao, D. Wang, A. Takemura, M. Uemura, K. Lin and Y. Xu, DOI: [10.1155/2019/8961409](https://doi.org/10.1155/2019/8961409).
- 33 S. Wei, J. X. Ma, L. Xu, X. S. Gu and X. L. Ma, *Mil. Med. Res.*, 2020, **7**, 54.
- 34 M. N. Rahaman, D. E. Day, B. Sonny Bal, Q. Fu, S. B. Jung, L. F. Bonewald and A. P. Tomsia, *Acta Biomater.*, 2011, **7**, 2355–2373.
- 35 W. Huang, M. N. Rahaman, D. E. Day and Y. Li, *Phys. Chem. Glasses: Eur. J. Glass Sci. Technol., Part B*, 2006, **47**, 647–658.
- 36 S. A. Hussein, R. Roshdy, M. S. A. El-sadek and M. Ezzeldien, *Optik*, 2022, **250**, 1–14.
- 37 R. G. Furlan, W. R. Correr, A. F. C. Russi, M. R. da Costa Iemma, E. Trovatti and É. Pecoraro, *J. Sol-Gel Sci. Technol.*, 2018, **88**, 181–191.
- 38 Q. Fu, M. N. Rahaman, H. Fu and X. Liu, *J. Biomed. Mater. Res., Part A*, 2010, **95**, 164–171.
- 39 X. Liu, M. N. Rahaman and D. E. Day, *J. Mater. Sci.: Mater. Med.*, 2013, **24**, 583–595.
- 40 J. Ning, A. Yao, D. Wang, W. Huang, H. Fu, X. Liu, X. Jiang and X. Zhang, *Mater. Lett.*, 2007, **61**, 5223–5226.
- 41 S. Jung, *Dr. Diss.*, 2010, 1–350.
- 42 A. M. Deliormanli, *Ceram. Int.*, 2013, **39**, 8087–8095.
- 43 H. Wang, S. Zhao, J. Zhou, Y. Shen, W. Huang, C. Zhang, M. N. Rahaman and D. Wang, *J. Mater. Chem. B*, 2014, **2**, 8547–8557.
- 44 H. Wang, S. Zhao, W. Xiao, J. Xue, Y. Shen, J. Zhou, W. Huang, M. N. Rahaman, C. Zhang and D. Wang, *Mater. Sci. Eng., C*, 2016, **58**, 194–203.
- 45 D. Zhao, W. Huang, M. N. Rahaman, D. E. Day and D. Wang, *Acta Biomater.*, 2009, **5**, 1265–1273.
- 46 R. Zhao, L. Shi, L. Gu, X. Qin, Z. Song, X. Fan, P. Zhao, C. Li, H. Zheng, Z. Li and Q. Wang, *J. Appl. Biomater. Funct. Mater.*, 2021, DOI: [10.1177/22808000211040910](https://doi.org/10.1177/22808000211040910).

47 F. H. Elbatal, M. A. Ouis and H. A. Elbatal, *Ceram. Int.*, 2016, **42**, 8247–8256.

48 N. Mutlu, F. Kurtuldu, I. Unalan, Z. Neščáková, H. Kaňková, D. Galusková, M. Michálek, L. Liverani, D. Galusek and A. R. Boccaccini, *Ceram. Int.*, 2022, **48**, 16404–16417.

49 S. Patel, R. K. Samudrala, S. Palakurthy, B. Manavathi, R. Gujjala and A. P. Azeem, *Ceram. Int.*, 2022, **48**, 12625–12634.

50 A. E. Omar, A. M. Ibrahim, T. H. Abd El-Aziz, Z. M. Al-Rashidy and M. M. Farag, *J. Biomed. Mater. Res., Part B*, 2021, **109**, 1059–1073.

51 S. Adepu and S. Ramakrishna, *Molecules*, 2021, **26**, 5905.

52 G. Kaur, O. P. Pandey, K. Singh, D. Homa, B. Scott and G. Pickrell, *J. Biomed. Mater. Res., Part A*, 2014, **102**, 254–274.

53 D. Ege, K. Zheng and A. R. Boccaccini, *ACS Appl. Bio Mater.*, 2022, **5**, 3608–3622.

54 S. Yamaguchi, *Bioact. Glas. Glas.*, 2022, 79–86.

55 A. Hoppe, V. Mouriño and A. R. Boccaccini, *Biomater. Sci.*, 2013, **1**, 254–256.

56 V. Mouriño, J. P. Cattalini and A. R. Boccaccini, DOI: [10.1098/rsif.2011.0611](https://doi.org/10.1098/rsif.2011.0611).

57 F. H. Nielsen, *Nutr. Rev.*, 2008, **66**, 183–191.

58 L. Pizzorno, *Integr. Med. A Clin. J.*, 2015, **14**, 35.

59 R. F. Moseman, *Environ. Health Perspect.*, 1994, **102**, 113.

60 M. Hubert and A. J. Faber, *Phys. Chem. Glasses: Eur. J. Glass Sci. Technol., Part B*, 2014, **55**, 136–158.

61 K. Schuhladen, U. Pantulap, K. Engel, P. Jeleň, Z. Olejniczak, L. Hupa, M. Sitarz and A. R. Boccaccini, *Int. J. Appl. Glas. Sci.*, 2021, **12**, 293–312.

62 S. A. R. Coelho, *Hybrid Organic-Inorganic Borosilicate Materials by Sol-Gel for Bone Tissue Engineering*, Universidade de Aveiro, 2018, <https://hdl.handle.net/10773/25818>.

63 A. C. Wright, *Phys. Chem. Glas.*, 2010, **51**, 1–39.

64 A. C. Wright, G. Dalba, F. Rocca and N. M. Vedishcheva, *Phys. Chem. Glasses: Eur. J. Glass Sci. Technol., Part B*, 2010, **51**, 233–265.

65 C. Gautam, A. K. Yadav and A. K. Singh, *ISRN Ceram.*, 2012, **2012**, 1–17.

66 J. E. Shelby, *Introd. to Glas. Sci. Technol.*, 2005, 72–110.

67 W. C. Lepry and S. N. Nazhat, *Mater. Adv.*, 2020, **1**, 1371–1381.

68 J. Wu, J. F. Stebbins and T. Rouxel, *J. Am. Ceram. Soc.*, 2014, **97**, 2794–2801.

69 A. R. Boccaccini, D. S. Brauer and L. Hupa, *Bioactive Glasses Series Editors: Titles in this Series*, 2017, pp. 61–88.

70 D. P. Button, R. Tandon, C. King, M. H. Veléz, H. L. Tuller and D. R. Uhlmann, *J. Non. Cryst. Solids*, 1982, **49**, 129–142.

71 D. L. Griscom, Borate Glass Structure, in *Borate Glasses: Structure, Properties, Applications*, ed. L. D. Pye, V. D. Fréchette and N. J. Kreidl, Plenum Press, New York, 1978.

72 S. Naseri, W. C. Lepry, V. B. Maisuria, N. Tufenkji and S. N. Nazhat, *J. Non-Cryst. Solids*, 2019, **505**, 438–446.

73 K. Rao, *Structural Chemistry of Glasses*, Elsevier, 2002.

74 Kristallstruktur Bortrioxid-Boron trioxide-Wikipedia, [https://en.wikipedia.org/wiki/Boron\\_trioxide#/media/File:Kristallstruktur\\_Bortrioxid.png](https://en.wikipedia.org/wiki/Boron_trioxide#/media/File:Kristallstruktur_Bortrioxid.png), (accessed 28 September 2022).

75 W. F. Du, K. Kuraoka, T. Akai and T. Yazawa, *J. Mater. Sci.*, 2000, **35**, 4865–4871.

76 Y. D. Yiannopoulos, G. D. Chryssikos and E. I. Kamitsos, *Phys. Chem. Glas.*, 2001, **42**, 164–172.

77 O. Rodriguez, A. Matinmanesh, S. Phull, E. Schemitsch, P. Zalzal, O. Clarkin, M. Papini and M. Towler, *J. Funct. Biomater.*, 2016, **7**, 32.

78 O. Rodriguez, D. J. Curran, M. Papini, L. M. Placek, A. W. Wren, E. H. Schemitsch, P. Zalzal and M. R. Towler, *J. Non. Cryst. Solids*, 2016, **433**, 95–102.

79 L. Deilmann, O. Winter, B. Cerrutti, H. Bradtmüller, C. Herzig, A. Limbeck, O. Lahayne, C. Hellmich, H. Eckert and D. Eder, *J. Mater. Chem. B*, 2020, **8**, 1456–1465.

80 M. Ojansivu, A. Mishra, S. Vanhatupa, M. Juntunen, A. Larionova, J. Massera and S. Miettinen, *PLoS One*, 2018, **13**, e0202740.

81 S. Decker, M. Arango-Ospina, F. Rehder, A. Moghaddam, R. Simon, C. Merle, T. Renkawitz, A. R. Boccaccini and F. Westhauser, *Sci. Rep.*, 2022, **12**, 8510.

82 N. W. Marion, W. Liang, G. C. Reilly, D. E. Day, M. N. Rahaman and J. J. Mao, *Mech. Adv. Mater. Struct.*, 2005, **12**, 239–246.

83 F. Westhauser, B. Widholz, Q. Nawaz, S. Tsitlakidis, S. Hagmann, A. Moghaddam and A. R. Boccaccini, *Biomater. Sci.*, 2019, **7**, 5161–5176.

84 K. A. Cole, G. A. Funk, M. N. Rahaman and T. E. McIff, *J. Biomed. Mater. Res., Part B*, 2020, **108**, 1580–1591.

85 D. Zhang, O. Leppäranta, E. Munukka, H. Ylänen, M. K. Viljanen, E. Eerola, M. Hupa and L. Hupa, *J. Biomed. Mater. Res., Part A*, 2010, **93**, 475–483.

86 A. Tilocca, *Proc. R. Soc. A Math. Phys. Eng. Sci.*, 2009, **465**, 1003–1027.

87 D. F. Williams, *Biomaterials*, 2008, **29**, 2941–2953.

88 L. L. Hench, *Ann. N. Y. Acad. Sci.*, 1988, **523**, 54–71.

89 A. J. Salinas and M. Vallet-Regí, *RSC Adv.*, 2013, **3**, 11116.

90 S. A. Bessedina, V. G. Konakov and M. M. Schultz, *Rev. Adv. Mater. Sci.*, 2002, **3**, 37–66.

91 F. Kracek and G. Morey, H. M.-A. J. S. A and U. 1938, earth.geology.yale.edu.

92 S. Sakka and J. D. Mackenzie, *J. Non. Cryst. Solids*, 1971, **6**, 145–162.

93 R. R. Shaw and D. R. Uhlmann, *J. Non. Cryst. Solids*, 1971, **5**, 237–263.

94 I. D. Thompson and L. L. Hench, *Proc. Inst. Mech. Eng., Part H*, 2016, **212**, 127–136.

95 H. F. Shermer, *J. Res. Natl. Bur. Stand.*, 1934, **56**, 73.

96 J. M. Gomez-Vega, E. Saiz, A. P. Tomsia, G. W. Marshall and S. J. Marshall, *Biomaterials*, 2000, **21**, 105–111.

97 L. Peddi, R. K. Brow and R. F. Brown, *J. Mater. Sci.: Mater. Med.*, 2008, **19**, 3145–3152.

98 O. Nilsson, O. Sandberg and G. Bäckström, *Int. J. Thermophys.*, 1985, **6**, 267–273.

99 A. K. Varshneya and J. C. Mauro, *Fundam. Inorg. Glas.*, 2019, 273–281.

100 B. San Miguel, R. Kriauciunas, S. Tosatti, M. Ehrbar, C. Ghayor, M. Textor and F. E. Weber, *J. Biomed. Mater. Res., Part A*, 2010, **94**, 1023–1033.

101 X. Cui, C. Zhao, Y. Gu, L. Li, H. Wang, W. Huang, N. Zhou, D. Wang, Y. Zhu, J. Xu, S. Luo, C. Zhang and M. N. Rahaman, *J. Mater. Sci.: Mater. Med.*, 2014, **25**, 733–745.

102 C. G. Pantano, A. E. Clark and L. L. Hench, *J. Am. Ceram. Soc.*, 1974, **57**, 412–413.

103 R. Chen, Q. Li, Q. Zhang, S. Xu, J. Han, P. Huang, Z. Yu, D. Jia, J. Liu, H. Jia, M. Shen, B. Hu, H. Wang, H. Zhan, T. Zhang, K. Ma and J. Wang, *Chem. Eng. J.*, 2021, **426**, 130299.

104 W. M. Abd-Allah and R. M. Fathy, *J. Biol. Inorg. Chem.*, 2022, **27**, 155–173.

105 M. N. Rahaman, D. E. Day, B. Sonny Bal, Q. Fu, S. B. Jung, L. F. Bonewald and A. P. Tomsia, *Acta Biomater.*, 2011, **7**, 2355–2373.

106 Y. Gu, W. Xiao, L. Lu, W. Huang, M. N. Rahaman and D. Wang, *J. Mater. Sci.*, 2010, **46**, 47–54.

107 H. G. McIlvried and F. E. Massoth, *Ind. Eng. Chem. Fundam.*, 1973, **12**, 225–229.

108 C. Pramanik, T. Wang, S. Ghoshal, L. Niu, B. A. Newcomb, Y. Liu, C. M. Primus, H. Feng, D. H. Pashley, S. Kumar and F. R. Tay, *J. Mater. Chem. B*, 2015, **3**, 959–963.

109 X. Liu, Z. Xie, C. Zhang, H. Pan, M. N. Rahaman, X. Zhang, Q. Fu and W. Huang, *J. Mater. Sci.: Mater. Med.*, 2010, **21**, 575–582.

110 A. Ewald, C. Käppel, E. Vorndran, C. Moseke, M. Gelinsky and U. Gbureck, *J. Biomed. Mater. Res., Part A*, 2012, **100A**, 2392–2400.

111 M. M. Erol, V. Mouriño, P. Newby, X. Chatzistavrou, J. A. Roether, L. Hupa and A. R. Boccaccini, *Acta Biomater.*, 2012, **8**, 792–801.

112 A. Hoppe, R. Meszaros, C. Stähli, S. Romeis, J. Schmidt, W. Peukert, B. Marelli, S. N. Nazhat, L. Wondraczek, J. Lao, E. Jallot and A. R. Boccaccini, *J. Mater. Chem. B*, 2013, **1**, 5659–5674.

113 C. Gérard, L. J. Bordeleau, J. Barralet and C. J. Doillon, *Biomaterials*, 2010, **31**, 824–831.

114 D. Bar-Or, G. W. Thomas, R. L. Yukl, L. T. Rael, R. P. Shimonkevitz, C. G. Curtis and J. V. Winkler, *Shock*, 2003, **20**, 154–158.

115 H. D. Schreiber, B. K. Kochanowski, C. W. Schreiber, A. B. Morgan, M. T. Coolbaugh and T. G. Dunlap, *J. Non. Cryst. Solids*, 1994, **177**, 340–346.

116 R. S. Abdurakhmanov, T. A. Ivanova, R. S. Abdurakhmanov and T. A. Ivanova, *JMoSt*, 1978, **46**, 229–244.

117 K. Schuhladen, X. Wang, L. Hupa and A. R. Boccaccini, *J. Non. Cryst. Solids*, 2018, **502**, 22–34.

118 J. N. Oliver, O. Akande, M. Ecker, J. N. Oliver, O. Akande and M. Ecker, DOI: [10.5772/INTECHOPEN.99430](https://doi.org/10.5772/INTECHOPEN.99430).

119 Y. Wang, W. Zhang and Q. Yao, *J. Orthop. Transl.*, 2021, **29**, 60–71.

120 L. Pang, R. Zhao, J. Chen, J. Ding, X. Chen, W. Chai, X. Cui, X. Li, D. Wang and H. Pan, *Bioact. Mater.*, 2022, **12**, 1–15.

121 S. Zhao, L. Li, H. Wang, Y. Zhang, X. Cheng, N. Zhou, M. N. Rahaman, Z. Liu, W. Huang and C. Zhang, *Biomaterials*, 2015, **53**, 379–391.

122 Y. Lin, W. Xiao, B. S. Bal and M. N. Rahaman, *Mater. Sci. Eng. C*, 2016, **67**, 440–452.

123 G. Jagan Mohini, N. Krishnamacharyulu, G. Sahaya Basakaran, P. Venkateswara Rao and N. Veeraiah, *Appl. Surf. Sci.*, 2013, **287**, 46–53.

124 J. Zhao, X. Xu, X. Chen, Q. Xu, Z. Luo, X. Qiao, J. Du, X. Fan and G. Qian, *J. Eur. Ceram. Soc.*, 2019, **39**, 5018–5029.

125 G. El Damrawi, A. M. Abdelghany and H. Salaheldin, *Bull. Chem. Soc. Ethiop.*, 2022, **36**, 597–606.

126 S. Bruns, T. Uesbeck, D. Weil, D. Möncke, L. van Wüllen, K. Durst and D. de Ligny, *Front. Mater.*, 2020, **7**, 189.

127 A. A. El-Kheshen, F. A. Khalifa, E. A. Saad and R. L. Elwan, *Ceram. Int.*, 2008, **34**, 1667–1673.

128 J. R. Jones, E. Gentleman and J. Polak, *Elements*, 2007, **3**, 393–399.

129 K. F. Frederiksen, K. Januchta, N. Mascaraque, R. E. Youngman, M. Bauchy, S. J. Rzoska, M. Bockowski and M. M. Smedskjaer, *J. Phys. Chem. B*, 2018, **122**, 6287–6295.

130 K. Bourhis, J. Massera, L. Petit, H. Ihlainen, A. Fargues, T. Cardinal, L. Hupa, M. Hupa, M. Dussauze, V. Rodriguez, C. Boussard-Plédel, B. Bureau, C. Roiland and M. Ferraris, *Mater. Res. Bull.*, 2015, **63**, 41–50.

131 T. Oey, K. F. Frederiksen, N. Mascaraque, R. Youngman, M. Balonis, M. M. Smedskjaer, M. Bauchy and G. Sant, *J. Non. Cryst. Solids*, 2019, **505**, 279–285.

132 N. Mascaraque, K. Januchta, K. F. Frederiksen, R. E. Youngman, M. Bauchy and M. M. Smedskjaer, *J. Am. Ceram. Soc.*, 2019, **102**, 1157–1168.

133 A. A. Osipov, V. E. Eremyshev, A. S. Mazur, P. M. Tolstoi and L. M. Osipova, *Glas. Phys. Chem.*, 2016, **42**, 230–237.

134 B. F. Boyce, H. Y. Elder, H. L. Elliot, I. Fogelman, G. S. Fell, B. J. Junor, G. Beastall and I. T. Boyle, *Lancet*, 1982, **2**, 1009–1013.

135 J. G. Joshi, *BioFactors*, 1990, **2**, 163–169.

136 G. Cournot-Witmer, J. Zingraff, J. J. Plachot, F. Escaig, R. Lefèvre, P. Boumati, A. Bourdeau, M. Garabédian, P. Galle, R. Bourdon, T. Drüeke and S. Balsan, *Kidney Int.*, 1981, **20**, 375–385.

137 M. C. Blades, D. P. Moore, P. A. Revell and R. Hill, *J. Mater. Sci. Mater. Med.*, 1998, **9**, 701–706.

138 C. Exley, *Morphologie*, 2016, **100**, 51–55.

139 A. Hoppe, N. S. Güldal and A. R. Boccaccini, *Biomaterials*, 2011, **32**, 2757–2774.

140 J. Isaac, J. Nohra, J. Lao, E. Jallot, J. M. Nedelec, A. Berdal and J. M. Sautier, *Eur. Cells Mater.*, 2011, **21**, 130–143.

141 P. Horák, M. Skácelová and A. Kazi, *J. Rheum. Dis. Treat.*, 2017, **3**, DOI: [10.23937/2469-5726/1510050](https://doi.org/10.23937/2469-5726/1510050).

142 P. Balasubramanian, T. Büttner, V. Miguez Pacheco and A. R. Boccaccini, *J. Eur. Ceram. Soc.*, 2018, **38**, 855–869.

143 H. Yin, C. Yang, Y. Gao, C. Wang, M. Li, H. Guo and Q. Tong, *J. Alloys Compd.*, 2018, **743**, 564–569.

144 H. B. Pan, X. L. Zhao, X. Zhang, K. B. Zhang, L. C. Li, Z. Y. Li, W. M. Lam, W. W. Lu, D. P. Wang, W. H. Huang,

K. L. Lin and J. Chang, *J. R. Soc., Interface*, 2010, **7**, 1025–1031.

145 X. Wu, G. Meng, S. Wang, F. Wu, W. Huang and Z. Gu, *Mater. Sci. Eng., C*, 2015, **52**, 242–250.

146 J. Buehler, P. Chappuis, J. L. Saffar, Y. Tsouderos and A. Vignery, *Bone*, 2001, **29**, 176–179.

147 X. Cui, Y. Zhang, J. Wang, C. Huang, Y. Wang, H. Yang, W. Liu, T. Wang, D. Wang, G. Wang, C. Ruan, D. Chen, W. W. Lu, W. Huang, M. N. Rahaman and H. Pan, *Bioact. Mater.*, 2020, **5**, 334–347.

148 C. Capuccini, P. Torricelli, F. Sima, E. Boanini, C. Ristoscu, B. Bracci, G. Socol, M. Fini, I. N. Mihailescu and A. Bigi, *Acta Biomater.*, 2008, **4**, 1885–1893.

149 Y. Zhu, Y. Ouyang, Y. Chang, C. Luo, J. Xu, C. Zhang and W. Huang, *Mol. Med. Rep.*, 2013, **7**, 1129–1136.

150 S. Peng, G. Zhou, K. D. K. Luk, K. M. C. Cheung, Z. Li, W. M. Lam, Z. Zhou and W. W. Lu, *Cell. Physiol. Biochem.*, 2009, **23**, 165–174.

151 P. J. Marie, D. Felsenberg and M. L. Brandi, *Osteoporos. Int.*, 2010, **22**, 1659–1667.

152 S. Peng, X. S. Liu, S. Huang, Z. Li, H. Pan, W. Zhen, K. D. K. Luk, X. E. Guo and W. W. Lu, *Bone*, 2011, **49**, 1290–1298.

153 Y. Li, W. Stone, E. H. Schemitsch, P. Zalzal, M. Papini, S. D. Waldman and M. R. Towler, *J. Biomater. Appl.*, 2016, **31**, 674–683.

154 Y. Wang, Q. Feng, Y. Chen, F. Wang and R. Song, *SSRN Electron. J.*, 2022, DOI: [10.2139/ssrn.4009614](https://doi.org/10.2139/ssrn.4009614).

155 Y. Zhang, X. Cui, S. Zhao, H. Wang, M. N. Rahaman, Z. Liu, W. Huang and C. Zhang, *ACS Appl. Mater. Interfaces*, 2015, **7**, 2393–2403.

156 J. Lao, J. M. Nedelec and E. Jallot, *J. Mater. Chem.*, 2009, **19**, 2940–2949.

157 S. Kargozar, M. Montazerian, E. Fiume and F. Baino, *Front. Bioeng. Biotechnol.*, 2019, **7**, 161.

158 Y. C. Fredholm, N. Karpukhina, D. S. Brauer, J. R. Jones, R. V. Law and R. G. Hill, *J. R. Soc., Interface*, 2012, **9**, 880–889.

159 F. G. Neto, R. D. S. Palácios, F. Sato, N. de, S. Fernandes, K. Miyuki, C. V. Nakamura, A. Steimacher and F. Pedrochi, *Materialia*, 2022, 101582.

160 A. W. Wren, A. Coughlan, C. M. Smith, S. P. Hudson, F. R. Laffir and M. R. Towler, *J. Biomed. Mater. Res., Part A*, 2015, **103**, 709–720.

161 L. M. Placek, T. J. Keenan, Y. Li, C. Yatongchai, D. Pradhan, D. Boyd, N. P. Mellott and A. W. Wren, *J. Biomed. Mater. Res., Part B*, 2016, **104**, 1703–1712.

162 J. Y. Wang, B. H. Wicklund, R. B. Gustilo and D. T. Tsukayama, *Biomaterials*, 1996, **17**, 2233–2240.

163 W. Q. Zhu, P. P. Ming, J. Qiu, S. Y. Shao, Y. J. Yu, J. X. Chen, J. Yang, L. N. Xu, S. M. Zhang and C. B. Tang, *J. Appl. Toxicol.*, 2018, **38**, 824–833.

164 M. Hashimoto, S. Kitaoka and H. Kanetaka, *Adv. Powder Technol.*, 2016, **27**, 2409–2415.

165 A. L. Raines, R. Olivares-Navarrete, M. Wieland, D. L. Cochran, Z. Schwartz and B. D. Boyan, *Biomaterials*, 2010, **31**, 4909–4917.

166 R. Shafaghi, O. Rodriguez, S. Phull, E. H. Schemitsch, P. Zalzal, S. D. Waldman, M. Papini and M. R. Towler, *Mater. Sci. Eng. C*, 2020, **107**, 110351.

167 R. Shafaghi, O. Rodriguez, A. W. Wren, L. Chiu, E. H. Schemitsch, P. Zalzal, S. D. Waldman, M. Papini and M. R. Towler, *J. Biomed. Mater. Res. A*, 2021, **109**, 146–158.

168 A. M. Deliormanli, *J. Mater. Sci. Mater. Med.*, 2015, **26**, 1–13.

169 N. Kamboj, A. Ressler and I. Hussainova, *Materials*, 2021, **14**, 5338.

170 M. I. Garchitorená and M. I. Garchitorená, *Odontoestomatologia*, 2019, **21**, 33–43.

171 T. Zhou, B. Sui, X. Mo and J. Sun, *Int. J. Nanomedicine*, 2017, **12**, 3495–3507.

172 J. Borrelly, M. F. Blech, G. Grosdidier, C. Martin-Thomas and P. Hartemann, *Ann. Chir. Plast. Esthet.*, 1991, **36**, 65–69.

173 B. Kaymaz, U. H. Gölgé, G. Ozylvacli, E. Kömürcü, F. Goksel, M. U. Mermerkaya and M. N. Doral, *Knee Surgery, Sport. Traumatol. Arthrosc.*, 2016, **24**, 3738–3744.

174 S. Demirci, A. Doğan, S. Aydin, E. Ç. Dülger and F. Şahin, *Mol. Cell. Biochem.*, 2016, **417**, 119–133.

175 R. M. Nzietchoueng, B. Dousset, P. Franck, M. Benderdour, P. Nabet and K. Hess, *J. Trace Elem. Med. Biol.*, 2002, **16**, 239–244.

176 M. Benderdour, K. Hess, M. Dzondo-Gadet, P. Nabet, F. Belleville and B. Dousset, *Biochem. Biophys. Res. Commun.*, 1998, **246**, 746–751.

177 M. Benderdour, T. Van Bui, K. Hess, A. Dicko, F. Belleville and B. Dousset, *J. Trace Elem. Med. Biol.*, 2000, **14**, 168–173.

178 D. G. Armstrong, D. P. Orgill, R. D. Galiano, P. M. Glat, L. A. DiDomenico, M. J. Carter and C. M. Zelen, *Int. Wound J.*, 2022, **19**, 791–801.

179 Borate-based bioactive glass improves treatment of diabetic foot ulcers - The American Ceramic Society, <https://ceramics.org/ceramic-tech-today/biomaterials/borate-based-bioactive-glass-improves-treatment-of-diabetic-foot-ulcers>, (accessed 20 July 2022).

180 H. S. Ryu, J. K. Lee, J. H. Seo, H. Kim, K. S. Hong, D. J. Kim, J. H. Lee, D. H. Lee, B. S. Chang, C. K. Lee and S. S. Chung, *J. Biomed. Mater. Res., Part A*, 2004, **68**, 79–89.

181 D. W. Buck, *Adv. Ski. Wound Care*, 2020, **33**, 1–6.

182 L. Sopchenski, S. Cogo, M. F. Dias-Ntipanyj, S. Elifio-Espósito, K. C. Popat and P. Soares, *Appl. Surf. Sci.*, 2018, **458**, 49–58.

183 M. Ottomeyer, A. Mohammadkhan, D. Day and D. Westenberg, *Adv. Microbiol.*, 2016, **6**, 776–787.

184 K. Schuhladen, S. N. V. Raghu, L. Liverani, Z. Neščáková and A. R. Boccaccini, *J. Biomed. Mater. Res., Part B*, 2021, **109**, 180–192.

185 K. R. Hixon, T. Lu, M. N. Carletta, S. H. McBride-Gagyi, B. E. Janowiak and S. A. Sell, *J. Biomed. Mater. Res. B. Appl. Biomater.*, 2018, **106**, 1918–1933.

186 S. Sadeghzade, R. Emadi and S. Labbaf, *Mater. Chem. Phys.*, 2017, **202**, 95–103.

187 A. A. El-Rashidy, J. A. Roether, L. Harhaus, U. Kneser and A. R. Boccaccini, *Acta Biomater.*, 2017, **62**, 1–28.

188 F. J. Murray, *Regul. Toxicol. Pharmacol.*, 1995, **22**, 221–230.

189 F. J. Murray, *Biol. Trace Elem. Res.*, 1998, **66**, 331–341.

190 F. H. Nielsen, *Environmental Health Perspectives*, Environ Health Perspect, 1994, vol. 102, pp. 59–63.

191 J. T. Mader, G. C. Landon and J. Calhoun, *Clin. Orthop. Relat. Res.*, 1993, **295**, 87–95.

192 J. Rivadeneira and A. Gorustovich, *J. Appl. Microbiol.*, 2017, **122**, 1424–1437.

193 K. Kanellakopoulou and E. J. Giamarellos-Bourboulis, *Drugs*, 2012, **59**, 1223–1232.

194 M. T. Cunha, M. A. Murça, S. Nigro, G. B. Klautau and M. J. C. Salles, *BMC Infect. Dis.*, 2018, **18**, 1–6.

195 X. Zhang, U. P. Wyss, D. Pichora and M. F. A. Goosen, *J. Pharm. Pharmacol.*, 1994, **46**, 718–724.

196 M. P. Ginebra, T. Traykova and J. A. Planell, *J. Controlled Release*, 2006, **113**, 102–110.

197 M. Itokazu, T. Ohno, T. Tanemori, E. Wada, N. Kato and K. Watanabe, *J. Med. Microbiol.*, 1997, **46**, 779–783.

198 J. Zhang, J. Guan, C. Zhang, H. Wang, W. Huang, S. Guo, X. Niu, Z. Xie and Y. Wang, *Biomed. Mater.*, 2015, **10**, 065011.

199 L. Bi, M. N. Rahaman, D. E. Day, Z. Brown, C. Samujh, X. Liu, A. Mohammadkhah, V. Dusevich, J. D. Eick and L. F. Bonewald, *Acta Biomater.*, 2013, **9**, 8015–8026.

200 X. Huang, X. Liu, Y. Shang, F. Qiao and G. Chen, *Biomed. Res. Int.*, 2020, 8787394.

201 J. M. Jukes, S. K. Both, A. Leusink, L. M. T. Sterk, C. A. Van Blitterswijk and J. De Boer, *Proc. Natl. Acad. Sci. U. S. A.*, 2008, **105**, 6840–6845.

202 S. P. Bruder and B. S. Fox, *Clin. Orthop. Relat. Res.*, 1999, **367**, S68–S83.

203 G. Tang, Z. Liu, Y. Liu, J. Yu, X. Wang, Z. Tan and X. Ye, *Front. Cell Dev. Biol.*, 2021, **9**, 665813.

204 N. Jafari, M. S. Habashi, A. Hashemi, R. Shirazi, N. Tanideh and A. Tamadon, *Biomater. Res.*, 2022, **26**, 1–15.

205 H. R. Fernandes, A. Gaddam, A. Rebelo, D. Brazete, G. E. Stan and J. M. F. Ferreira, *Materials*, 2018, **11**, 2530.

206 E. E. Stroganova, N. Y. Mikhailenko and O. A. Moroz, *Glas. Ceram.*, 2003, **60**, 315–319.

207 L. L. Hench, *J. Am. Ceram. Soc.*, 1998, **81**, 1705–1728.

208 M. D. O'Donnell, *Acta Biomater.*, 2011, **7**, 2264–2269.

209 R. I. M. Asri, W. S. W. Harun, M. Samykano, N. A. C. Lah, S. A. C. Ghani, F. Tarlochan and M. R. Raza, *Mater. Sci. Eng., C*, 2017, **77**, 1261–1274.

210 S. Minagar, C. C. Berndt, J. Wang, E. Ivanova and C. Wen, *Acta Biomater.*, 2012, **8**, 2875–2888.

211 Y. Su, I. Cockerill, Y. Zheng, L. Tang, Y. X. Qin and D. Zhu, *Bioact. Mater.*, 2019, **4**, 196–206.

212 H. S. Coskun, L. Kehribar, S. Surucu, M. Aydin and M. Mahirogullari, *Cureus*, 2022, **14**, 1–7.

213 X. Zhang, W. T. Jia, Y. F. Gu, W. Xiao, X. Liu, D. P. Wang, C. Q. Zhang, W. H. Huang, M. N. Rahaman, D. E. Day and N. Zhou, *Biomaterials*, 2010, **31**, 5865–5874.

214 A. C. Profeta, *Dent. Mater. J.*, 2014, **33**, 443–452.

215 A. L. B. Maçón, E. M. Valliant, J. S. Earl and J. R. Jones, *Biomed. Glas.*, 2015, **1**, 41–50.

216 W. Li and A. R. Boccaccini, *Hot Top. Biomater.*, 2014, 56–68.

217 X. Qi, H. Wang, Y. Zhang, L. Pang, W. Xiao, W. Jia, S. Zhao, D. Wang, W. Huang and Q. Wang, *Int. J. Biol. Sci.*, 2018, **14**, 471–484.

218 E. Piatti, E. Verné and M. Miola, *Ceram. Int.*, 2022, **48**, 13706–13718.

219 A. M. Abdelghany, N. Mahmoud, Y. Abdou and F. El-Husseiny, *Biointerface Res. Appl. Chem.*, 2022, **13**, 19.

220 F. G. Neto, R. da, S. Palácios, F. Sato, N. de, S. Fernandes, K. Miyuki, C. V. Nakamura, A. Steimacher and F. Pedrochi, *Materialia*, 2022, **26**, 101582.

221 Z. M. Al-Rashidy, A. E. Omar, T. H. A. El-Aziz and M. M. Farag, *J. Inorg. Organomet. Polym. Mater.*, 2020, **30**, 3953–3964.

222 J. Isaac, J. Nohra, J. Lao, E. Jallot, J. M. Nedelec, A. Berdal and J. M. Sautier, *Eur. Cell. Mater.*, 2011, **21**, 130–143.

223 R. Chen, L. Sun, R. Tan, S. Xu, H. Xu, X. Zhao, T. Tao, Q. Zhang, H. Xia, J. Han, C. Liu, Z. Yu, H. Zhan, K. Ma and J. Wang, *Ceram. Int.*, 2022, **49**, 773–782.

224 H. Hu, Y. Tang, L. Pang, C. Lin, W. Huang, D. Wang and W. Jia, *ACS Appl. Mater. Interfaces*, 2018, **10**, 22939–22950.

225 Q. Yang, S. Chen, H. Shi, H. Xiao and Y. Ma, *Mater. Sci. Eng., C*, 2015, **55**, 105–117.

226 J. Zhou, H. Wang, S. Zhao, N. Zhou, L. Li, W. Huang, D. Wang and C. Zhang, *Mater. Sci. Eng. C*, 2016, **60**, 437–445.

227 A. Mehrabi, A. Karimi, S. Mashayekhan, A. Samadikuchaksaraei and P. B. Milan, *Int. J. Biol. Macromol.*, 2022, **222**, 620–635.

228 J. V. Rau, A. De Bonis, M. Curcio, K. Schuhladen, K. Barbaro, G. De Bellis, R. Teghil and A. R. Boccaccini, *Coatings*, 2020, **10**, 1–13.

229 R. M. Rad, Borate modified bioglass containing scaffolds for dental tissue engineering applications, PhD thesis, Middle East Technical University, 2018.